

New aspect of chiral $SU(2)$ and $U(1)$ axial breaking in QCD

Chuan-Xin Cui,^{*} Jin-Yang Li,[†] and Shinya Matsuzaki[‡]

Center for Theoretical Physics and College of Physics, Jilin University, Changchun, 130012, China

Mamiya Kawaguchi[§]

School of Nuclear Science and Technology, University of Chinese Academy of Sciences, Beijing 100049, China

Akio Tomiya[¶]

*Department of Information Technology, International Professional University of Technology in Osaka,
3-3-1 Umeda, Kita-Ku, Osaka, 530-0001, Japan*

Violation of the $U(1)$ axial symmetry in QCD is stricter than the chiral $SU(2)$ breaking, simply because of the presence of the quantum axial anomaly. If the QCD gauge coupling is sent to zero (the asymptotic free limit, where the $U(1)$ axial anomaly does not exist), the strength of the $U(1)$ axial breaking coincides with that of the chiral $SU(2)$ breaking, which we shall in short call an axial-chiral coincidence. This coincidence is *trivial* since QCD then becomes a non-interacting theory. Actually, there exists another limit in the QCD parameter space, where an axial-chiral coincidence occurs even with nonzero QCD gauge coupling, that can be dubbed a *nontrivial* coincidence: it is the case with the massive light quarks ($m_l \neq 0$) and the massless strange quark ($m_s = 0$), due to the flavor-singlet nature of the topological susceptibility. This coincidence is robust and tied to the anomalous chiral Ward-Takahashi identity, which is operative even at hot QCD. This implies that the chiral $SU(2)$ symmetry is restored simultaneously with the $U(1)$ axial symmetry at high temperatures. This simultaneous restoration is independent of $m_l (\neq 0)$, hence is irrespective to the order of the chiral phase transition. In this paper, we discuss how the real-life QCD can be evolved from the nontrivial chiral-axial coincidence limit, by working on a Nambu-Jona-Lasinio model with the $U(1)$ axial anomaly contribution properly incorporated. It is shown that at high temperatures the large differences between the restorations of the chiral $SU(2)$ symmetry and the $U(1)$ axial symmetry for two light quarks and a sufficiently large current mass for the strange quark is induced by a significant interference of the topological susceptibility. Thus the deviation from the nontrivial coincidence, which is monitored by the strange quark mass controlling the topological susceptibility, provides a new way of understanding the chiral $SU(2)$ and $U(1)$ axial breaking in QCD.

PACS numbers:

I. INTRODUCTION

The $U(1)$ axial symmetry in QCD (denoted as $U(1)_A$) is explicitly broken by gluonic quantum corrections, called the $U(1)_A$ anomaly (or the axial anomaly), as well as by the current quark masses. The axial anomaly survives even in the limit of massless quarks. Thereby the $U(1)_A$ anomaly is anticipated to significantly interfere with the spontaneous breaking of the $SU(2)$ axial (referred to as chiral $SU(2)$) symmetry in the nonperturbative QCD vacuum, i.e., the quark condensate, hence affecting the chiral phase transition in hot QCD.

As a pioneer work based on the renormalization group running in a chiral effective model, Pisarski and Wilczek [1] pointed out that the $U(1)_A$ anomaly, as well as the number of the quark-flavors, affect the order of the chiral phase transition in massless QCD. Based on this, the order of the chiral phase transition depending on the quark flavors has extensively been explored in lattice QCD in terms of the universality class [2–7]. The chiral phase transition is mapped onto a phase diagram in the quark mass plane, called the Columbia plot [8]. However, the anomalous $U(1)_A$ contribution to the whole phase diagram has not been clarified yet.

Though there is no definite order parameter, the strength of the $U(1)_A$ breaking can be indicated by meson correlation functions χ_{meson} (susceptibility functions) for the $U(1)_A$ partners within the $U(2)$ meson quartet: χ_σ and

^{*}cuicx1618@mails.jlu.edu.cn

[†]lijy1118@mails.jlu.edu.cn

[‡]synya@jlu.edu.cn

[§]mamiya@ucas.ac.cn

[¶]akio@yukawa.kyoto-u.ac.jp

χ_η for (σ, η) mesons, and χ_π and χ_δ for (π, δ) mesons. Those meson susceptibility functions are transformed also by the chiral $SU(2)$ rotation, like $(\chi_\sigma, \chi_\eta) \leftrightarrow (\chi_\pi, \chi_\delta)$ [See also Eq.(2)]. However, there exists a discrepancy between the meson susceptibility functions for the chiral symmetry, $\chi_\sigma \approx \chi_\pi$ and $\chi_\delta \approx \chi_\eta$, and the axial symmetry, $\chi_\sigma \approx \chi_\eta$ and $\chi_\delta \approx \chi_\pi$, due to the spontaneous chiral symmetry breaking entangled with the $U(1)_A$ anomaly. Hence, the meson susceptibility functions cannot generically disentangle the $U(1)_A$ anomaly contribution from the contribution due to spontaneous chiral breaking.

With the increase of the temperature, the meson susceptibility functions for the chiral partners turn to be degenerate, as a consequence of the chiral restoration, $\chi_\sigma \sim \chi_\pi$ and $\chi_\delta \sim \chi_\eta$, where the spontaneous breaking strength is separated out. Similarly, the approximate axial restoration can be seen from the degeneracy of the axial partner in the meson susceptibility functions: $\chi_\sigma \sim \chi_\eta$ and $\chi_\pi \sim \chi_\delta$. Those degeneracies has been observed in the lattice QCD simulations with 2 + 1 flavors at physical quark masses [9, 10]. In this context, lattice QCD has also shown that the chiral symmetry tends to be restored faster than the $U(1)_A$ symmetry at around the (pseudo)critical temperature [9, 10]. This discrepancy between the chiral and axial symmetry restorations would be caused by the existence of the $U(1)_A$ anomaly, and this might be the role of $U(1)_A$ anomaly in the spontaneous breaking of the chiral symmetry. Furthermore, even if the light quarks become massless and the strange quark mass takes the physical value, the $U(1)_A$ anomaly contribution remains manifest in the meson susceptibility functions at high temperatures [11].

However, in contrast to the 2 + 1 flavor QCD, it has been discussed that within the two-flavor QCD at the chiral limit, the $U(1)_A$ anomaly does not affect the symmetry restoration [12–16]. Therefore, it is still unclear how the $U(1)_A$ anomaly could contribute to the chiral breaking in terms of quark-flavor and mass dependencies.

Another important aspect regarding the $U(1)_A$ anomaly that one should note is the close correlation with the transition rate of the topological charge of the vacuum, i.e., the topological susceptibility χ_{top} . Reflecting the flavor singlet nature of the QCD θ -vacuum [17, 18], χ_{top} is given as the sum of the quark condensates coupled to the current quark masses and pseudoscalar susceptibilities [19]: χ_{top} vanishes if either of quarks get massless. It is interesting to note that χ_{top} can be rewritten as the meson susceptibility functions $\chi_\pi, \chi_{\delta(\sigma)}$, and χ_η , by using the anomalous Ward-Takahashi identity for the chiral symmetry with three quark flavors [19–22] as $\chi_\eta - \chi_{\delta/\sigma} = \chi_\pi - \chi_{\delta/\sigma} + 4\chi_{\text{top}}/m_l^2$ [23], where m_l denotes the current mass of the up and down quarks. Note that the susceptibility difference on both sides of this identity plays the role of indicators of the breaking strength of the chiral or axial symmetry. This identity shows that χ_{top} is also important to explain the chiral and axial symmetry restorations through the meson susceptibility functions.

The transparent link of χ_{top} with the chiral or axial breaking can be observed in another way: it is seen through the Veneziano-Witten formula based on the current algebra assumed for $U(1)_A$ symmetry [24, 25], $m_\eta^2 f_\eta^2 \sim \chi_{\text{top,g}}$ where $\chi_{\text{top,g}}$ is the contribution of pure gluonic diagrams. Though it is formulated in the large N_c approximation for massless quarks (with N_c being the number of colors), the aspect of the formula makes transparent that at high temperatures, the smooth decrease of the topological susceptibility is a combined effect of melting of the chiral condensate (supposed to be scaled along with f_η) and suppression of the anomalous contribution to the mass of the isosinglet η , m_η (in the heavy quark limit).

Anyhow, it is true that if the gluonic $U(1)_A$ anomaly is removed, the strength of the chiral symmetry breaking will coincide with the strength of the axial symmetry breaking in the meson susceptibility functions. This corresponds to merely a trivial limit of QCD (with the gauge coupling sent to zero), in which the understanding of the symmetry restoration will obviously become transparent. However, the gluonic $U(1)_A$ anomaly is essential in the underlying QCD as an interacting gauge theory, so that its contribution would inevitably produce the intricate restoration phenomena involving contamination of the chiral and axial breaking, as mentioned above.

Therefore, in this paper, we focus on another limit where a nontrivial axial-chiral coincidence occurs even with nonzero QCD gauge coupling. The case we consider here is the one of massive light quarks ($m_l \neq 0$) and amassless strange quark ($m_s = 0$), due to the flavor-singlet nature of the topological susceptibility. Following a robust anomalous chiral Ward-Takahashi identity, this nontrivial coincidence is valid even at finite temperatures, so that the chiral symmetry gets restored simultaneously with the $U(1)_A$ symmetry at high temperatures, no matter what order of the chiral phase transition is performed.

Usually, the topological susceptibility is used as a probe for the effective restoration of the $U(1)$ axial symmetry when the chiral $SU(2)$ symmetry is restored at high temperatures. This is the way the differences in the restorations of chiral $SU(2)$ and $U(1)$ axial symmetries can be monitored by the temperature dependence of the topological susceptibility. However, this ordinary approach suffers from the practical difficulty to access the origin of the split without ambiguity, because the chiral $SU(2)$ symmetry breaking is highly contaminated with the $U(1)$ axial symmetry breaking even at the beginning, at the vacuum.

In contrast to the ordinary approach under the temperature control, the nontrivial coincidence discussed in the present paper provides a new approach: it is the strange quark mass that controls the strengths of the chiral $SU(2)$ symmetry breaking and the $U(1)$ axial symmetry breaking, and those strengths coincide in the limit $m_s = 0$.

Thus, the gap between the breaking strengths of the chiral $SU(2)$ and $U(1)$ axial symmetries is handled by the

strange quark mass, as it is the case for the $U(1)_A$ anomaly. This can be thought of as an alternative to large- N_c QCD a la Veneziano and Witten, as our approach uses fixed $N_c = 3$ and varies the current quark masses.

To understand the real-life QCD departing from the nontrivial coincidence limit, we employ the Nambu-Jona-Lasinio (NJL) model. We first confirm that the NJL model surely provides the nontrivial coincidence at the massless limit of the strange quark. Once the strange quark gets massive, the strange quark mass handles the deviation from the nontrivial coincidence. We explain how the large differences in the restorations of the chiral $SU(2)$ symmetry and the $U(1)_A$ symmetry for 2 + 1 flavors with physical quark masses is generated by a sufficiently large current mass of the strange quark through the significant interference of the topological susceptibility.

The deviation from the nontrivial coincidence as monitored by the strange quark mass by controlling the topological susceptibility provides a new way of understanding of the chiral and axial breaking in QCD, seen on the graphical description given by the Columbia plot.

II. COINCIDENCE BETWEEN CHIRAL AND AXIAL SYMMETRY BREAKING

As noted in the Introduction, the meson susceptibility function plays the role of an indicator for the chiral $SU(2)$ symmetry breaking and the $U(1)$ axial symmetry breaking. The $U(1)_A$ anomaly potentially produces a difference between the strength of the chiral symmetry breaking and the axial symmetry breaking in the meson susceptibility functions of the vacuum. In this section, we show that even in keeping a nonzero $U(1)_A$ anomaly, there generically exists the nontrivial coincidence between the chiral and axial symmetry breaking in QCD for $N_f = 2 + 1$ flavors.

A. Chiral and axial symmetry in meson susceptibility functions

We begin by introducing the scalar- and pseudoscalar-meson susceptibilities. The pion susceptibility χ_π , the η -meson susceptibility χ_η , the δ -meson susceptibility χ_δ (also known as a_0 meson), and the σ -meson susceptibility χ_σ are defined respectively as

$$\begin{aligned}\chi_\pi &= \int_T d^4x \left[\langle (i\bar{u}(0)\gamma_5 u(0))(i\bar{u}(x)\gamma_5 u(x)) \rangle_{\text{conn}} + \langle (i\bar{d}(0)\gamma_5 d(0))(i\bar{d}(x)\gamma_5 d(x)) \rangle_{\text{conn}} \right], \\ \chi_\eta &= \int_T d^4x \left[\langle (i\bar{u}(0)\gamma_5 u(0))(i\bar{u}(x)\gamma_5 u(x)) \rangle + \langle (i\bar{d}(0)\gamma_5 d(0))(i\bar{d}(x)\gamma_5 d(x)) \rangle + 2\langle (i\bar{u}(0)\gamma_5 u(0))(i\bar{d}(x)\gamma_5 d(x)) \rangle \right], \\ \chi_\delta &= \int_T d^4x \left[\langle (\bar{u}(0)u(0))(\bar{u}(x)u(x)) \rangle_{\text{conn}} + \langle (\bar{d}(0)d(0))(\bar{d}(x)d(x)) \rangle_{\text{conn}} \right], \\ \chi_\sigma &= \int_T d^4x \left[\langle (\bar{u}(0)u(0))(\bar{u}(x)u(x)) \rangle + \langle (\bar{d}(0)d(0))(\bar{d}(x)d(x)) \rangle + 2\langle (\bar{u}(0)u(0))(\bar{d}(x)d(x)) \rangle \right],\end{aligned}\quad (1)$$

where u and d are the up- and down-quark fields; $\langle \dots \rangle_{\text{conn}}$ represents the connected-graph part of the correlation function; $\int_T d^4x \equiv \int_0^{1/T} d\tau \int d^3x$ with the imaginary time $\tau = ix_0$. Under the chiral $SU(2)$ rotation and the $U(1)_A$ rotation, the meson susceptibility functions can be exchanged with each other:

$$\begin{aligned}\text{Chiral } SU(2) \text{ rotation : } & \begin{cases} \chi_\delta \leftrightarrow \chi_\eta \\ \chi_\sigma \leftrightarrow \chi_\pi \end{cases}, \\ U(1)_A \text{ rotation} & \begin{cases} \chi_\delta \leftrightarrow \chi_\pi \\ \chi_\sigma \leftrightarrow \chi_\eta \end{cases}.\end{aligned}\quad (2)$$

For the convenience of the reader, we also provide the following cartoon in order to visualize the chiral $SU(2)$ and $U(1)_A$ transformations for the meson susceptibility functions,

$$\begin{array}{ccc} & \xrightarrow{SU(2)} & \\ \chi_\pi & \longleftrightarrow & \chi_\sigma \\ \uparrow U(1)_A & & \uparrow U(1)_A \\ \chi_\delta & \longleftrightarrow & \chi_\eta \\ & \xrightarrow{SU(2)} & \end{array}$$

Since the meson susceptibility functions are linked with each other via the chiral symmetry and the axial symmetry, the chiral and axial partners become (approximately) degenerate, respectively, at the restoration limits of the chiral $SU(2)$ symmetry and the $U(1)_A$ symmetry:

$$\begin{aligned} \text{Chiral } SU(2) \text{ symmetric limit : } & \begin{cases} \chi_{\eta-\delta} = \chi_\eta - \chi_\delta \rightarrow 0 \\ \chi_{\pi-\sigma} = \chi_\pi - \chi_\sigma \rightarrow 0 \end{cases} , \\ U(1)_A \text{ symmetric limit : } & \begin{cases} \chi_{\pi-\delta} = \chi_\pi - \chi_\delta \rightarrow 0 \\ \chi_{\eta-\sigma} = \chi_\eta - \chi_\sigma \rightarrow 0 \end{cases} . \end{aligned} \quad (3)$$

Note that in the chiral limit, we encounter the infrared divergence in the pseudoscalar-meson susceptibilities due to the emergence of the exactly massless Nambu-Goldstone bosons. The nonzero light quark mass thus plays the role of a regulator for the infrared divergence, making them well-defined. The differences of the susceptibility functions of the mesons forming the chiral and axial partners, $\chi_{\eta-\delta}$, $\chi_{\pi-\sigma}$, $\chi_{\pi-\delta}$, and $\chi_{\eta-\sigma}$, can safely serve as well-defined indicators for the symmetry breaking of $SU(2)_L \times SU(2)_R$ and $U(1)_A$.

The pseudoscalar susceptibility functions have close correlations with the quark condensates through the anomalous Ward-Takahashi identities for the chiral symmetry with the three quark flavors [19, 20]:

$$\begin{aligned} \langle \bar{u}u \rangle + \langle \bar{d}d \rangle &= -m_l \chi_\pi , \\ \langle \bar{u}u \rangle + \langle \bar{d}d \rangle + 4\langle \bar{s}s \rangle &= -[m_l \chi_\eta - 2(m_s + m_l)(\chi_P^{us} + \chi_P^{ds}) + 4m_s \chi_P^{ss}] , \\ \langle \bar{u}u \rangle + \langle \bar{d}d \rangle - 2\langle \bar{s}s \rangle &= -[m_l \chi_\eta + (m_l - 2m_s)(\chi_P^{us} + \chi_P^{ds}) - 2m_s \chi_P^{ss}] , \end{aligned} \quad (4)$$

where $m_l = m_u = m_d$ is the isospin-symmetric mass for the up- and down quarks, m_s is the strange quark mass, and the pseudoscalar susceptibilities $\chi_P^{f_1 f_2}$, are defined as

$$\chi_P^{f_1 f_2} = \int_T d^4x \langle (\bar{q}_{f_1}(0) i\gamma_5 q_{f_1}(0)) (\bar{q}_{f_2}(x) i\gamma_5 q_{f_2}(x)) \rangle , \quad \text{for } q_{f_{1,2}} = u, d, s. \quad (5)$$

In addition, we also define the scalar susceptibilities $\chi_S^{f_1 f_2}$,

$$\chi_S^{f_1 f_2} = \int_T d^4x \langle (\bar{q}_{f_1}(0) q_{f_1}(0)) (\bar{q}_{f_2}(x) q_{f_2}(x)) \rangle. \quad (6)$$

Due to the the anomalous Ward-Takahashi identities in Eq. (4), the behavior of the quark condensates close to the chiral phase transition is directly reflected in that of the pseudoscalar susceptibility functions.

B. Trivial coincidence between chiral and axial symmetry breaking

In the previous subsection, we have shown that $\chi_{\eta-\delta}$ or $\chi_{\pi-\sigma}$ ($\chi_{\pi-\delta}$ or $\chi_{\eta-\sigma}$) serves as an indicator for the strength of the chiral (axial) symmetry breaking. The symmetry breaking in the meson susceptibility functions has been studied in a chiral-effective model approach [20, 23] and the first-principle calculations of lattice QCD [9, 10, 12, 13, 21, 22]. It is known that there exists a difference between the indicators for the chiral $SU(2)_L \times SU(2)_R$ symmetry breaking and the $U(1)_A$ symmetry breaking at the vacuum:

$$\begin{cases} \chi_{\eta-\delta} \neq \chi_{\pi-\delta} \\ \chi_{\pi-\sigma} \neq \chi_{\eta-\sigma} \end{cases} . \quad (7)$$

This discrepancy is originated from the anomalous current conservation laws for the $U(1)_A$ symmetry. In the underlying QCD, the chiral current $j_A^{a\mu}$ and the axial current j_A^μ follow the following anomalous conservation laws:

$$\begin{aligned} \partial_\mu j_A^{a\mu} &= i\bar{q} \left\{ \mathbf{m}, \frac{\tau^a}{2} \right\} \gamma_5 q , \\ \partial_\mu j_A^\mu &= 2i\bar{q} \mathbf{m} \gamma_5 q + N_f \frac{g^2}{32\pi^2} \epsilon^{\mu\nu\rho\sigma} F_{\mu\nu}^a F_{\rho\sigma}^a , \end{aligned} \quad (8)$$

where q is the $SU(3)$ -flavor triplet-quark field $q = (u, d, s)^T$; the chiral current and the axial current are defined as $j_A^{a\mu} = \bar{q} \gamma_\mu \gamma_5 \frac{\tau^a}{2} q$ and $j_A^\mu = \bar{q} \gamma_5 \gamma^\mu q$, respectively; τ^a ($a = 1, 2, 3$) generate an $SU(2)$ subalgebra of Gell-Mann matrices;

\mathbf{m} denotes the mass matrix $\mathbf{m} = \text{diag}(m_u, m_d, m_s)$; $F_{\mu\nu}^a$ denotes the field strength of the gluon field; g stands for the QCD coupling constant. At the Lagrangian level, the chiral $SU(2)$ symmetry and the $U(1)_A$ symmetry are explicitly broken by the current quark mass terms, so that the chiral current and the axial current get anomalous parts from the quark mass terms in Eq. (8). These anomalous parts of the quark masses can be tuned to vanish by taking the chiral limit $\mathbf{m} = 0$.

Looking at the QCD generating functional, one notices that the gluonic quantum anomaly $g^2 \epsilon^{\mu\nu\rho\sigma} F_{\mu\nu}^a F_{\rho\sigma}^a$ arises in the axial current, but not in the chiral current. The quantum correction only to the $U(1)_A$ symmetry induces the sizable discrepancy between the chiral symmetry breaking and the axial symmetry breaking in Eq (7). In contrast to the anomalous term of the quark mass, the quantum gluonic anomaly cannot be eliminated from Eq. (8) by tuning the external parameters like the current quark masses. If one tries to remove the gluonic quantum anomaly in Eq. (8), the QCD coupling constant would be taken as $g = 0$. The vanishing quantum anomaly provides the coincidence between the strength of the chiral symmetry breaking and the axial symmetry breaking in the meson susceptibility functions^{#1}:

$$\begin{cases} \chi_{\eta-\delta} = \chi_{\pi-\delta} \\ \chi_{\pi-\sigma} = \chi_{\eta-\sigma} \end{cases} \quad (\text{for } g = 0). \quad (9)$$

However, in this case QCD obviously becomes a free theory and loses the nontrivial features driven by the interaction among quarks and gluons as quantum field theory.

C. Flavor singlet nature of topological susceptibility

We will explain later that the discrepancy between the meson susceptibility functions in Eq. (7) is actually responsible for nonzero topological susceptibility. To make it better understood, in this subsection we give a brief review of the construction of the topological susceptibility [19] and its flavor singlet nature.

The topological susceptibility is a quantity to measure the topological charge fluctuation of the QCD- θ vacuum, which is defined as the curvature of the θ -dependent QCD vacuum energy $V(\theta)$ at $\theta = 0$,

$$\chi_{\text{top}} = - \int_T d^4x \frac{\delta^2 V(\theta)}{\delta\theta(x)\delta\theta(0)} \Big|_{\theta=0}. \quad (10)$$

$V(\theta)$ represents the effective potential of QCD, which includes the QCD θ -term represented by the flavor-singlet gluonic operator, $\theta g^2 \epsilon^{\mu\nu\rho\sigma} F_{\mu\nu}^a F_{\rho\sigma}^a$:

$$\begin{aligned} V(\theta) &= -\log Z_{\text{QCD}}(\theta), \\ Z_{\text{QCD}}(\theta) &= \int [\Pi_f dq_f d\bar{q}_f][dA] \exp \left[- \int_T d^4x \left\{ \sum_{f=u,d,s} \left(\bar{q}_L^f i\gamma^\mu D_\mu q_L^f + \bar{q}_R^f i\gamma^\mu D_\mu q_R^f \right. \right. \right. \\ &\quad \left. \left. \left. + \bar{q}_L^f m_f q_R^f + \bar{q}_R^f m_f q_L^f \right) + \frac{1}{4} (F_{\mu\nu}^a)^2 + \frac{i\theta}{32\pi^2} g^2 F_{\mu\nu}^a \tilde{F}_{\mu\nu}^a \right\} \right] \end{aligned} \quad (11)$$

with Z_{QCD} being the generating functional of QCD in Euclidean space. In Eq.(11) $q_{L(R)}^f$ denote the left- (right-) handed quark fields; the covariant derivative of the quark field is represented as D_μ involving the gluon fields (A_μ^a) and $F_{\mu\nu}^a$ is the field strength of the gluon field. From Eq. (10), the topological susceptibility χ_{top} is directly given as

$$\chi_{\text{top}} = \int_T d^4x \langle Q(x)Q(0) \rangle \quad (12)$$

with $Q = g^2/(32\pi^2) F_{\mu\nu}^a \tilde{F}^{a\mu\nu}$. Obviously the topological susceptibility in Eq. (12) takes a flavor-independent form.

^{#1} In the free theory of quarks, the chiral symmetry is not spontaneously broken, so that the $U(2)_L \times U(2)_R$ symmetry is realized in the meson susceptibility functions: $\chi_\pi = \chi_\sigma = \chi_\eta = \chi_\delta$ for $g = 0$.

Under the $U(1)_A$ transformation with the rotation angles $\theta_{f=u,d,s}$, the QCD- θ term in the generating functional is shifted by the $U(1)_A$ anomaly:

$$\int [\Pi_f dq_f d\bar{q}_f][dA] \exp \left[- \int_T d^4x \left\{ \sum_{f=u,d,s} \left(\bar{q}_L^f i\gamma^\mu D_\mu q_L^f + \bar{q}_R^f i\gamma^\mu D_\mu q_R^f + \bar{q}_L^f m_f e^{i\theta_f} q_R^f + \bar{q}_R^f m_f e^{-i\theta_f} q_L^f \right) + \frac{1}{4} (F_{\mu\nu}^a)^2 + \frac{i(\theta - \bar{\theta})}{32\pi^2} g^2 F_{\mu\nu}^a \tilde{F}_{\mu\nu}^a \right\} \right], \quad (13)$$

where $\bar{\theta} = \sum_{f=u,d,s} \theta_f = \theta_u + \theta_d + \theta_s$. The θ -dependence of the topological operator $F\tilde{F}$ can be transferred to the quark mass terms by choosing the rotation angles as

$$\bar{\theta} = \theta_u + \theta_d + \theta_s = \theta. \quad (14)$$

Absorbing the θ dependence into the quark mass terms by this choice, the QCD θ -term is removed from the generating functional. However, currently the θ -dependent quark mass term is not flavor universal, though the original QCD θ -term is flavor independent. Thus one should impose a flavor-singlet constraint on the axial rotation angles left in the quark mass sector as [17, 18]

$$m_u \theta_u = m_d \theta_d = m_s \theta_s, \quad (15)$$

for $\theta \ll 1$, so that the θ -dependent part of the quark mass term satisfies the flavor singlet nature:

$$\mathcal{L}_{\text{QCD}}^{(\theta)} = \sum_f \left(\bar{q}_L^f i\gamma^\mu D_\mu q_L^f + \bar{q}_R^f i\gamma^\mu D_\mu q_R^f \right) + \bar{q}_L \mathcal{M}_\theta q_R + \bar{q}_R \mathcal{M}_\theta^\dagger q_L + \frac{1}{4} (F_{\mu\nu}^a)^2, \quad (16)$$

where \mathcal{M}_θ denotes the θ -dependent quark matrix,

$$\mathcal{M}_\theta = \text{diag} \left[m_u \exp \left(i \frac{\bar{m}}{m_u} \theta \right), m_d \exp \left(i \frac{\bar{m}}{m_d} \theta \right), m_s \exp \left(i \frac{\bar{m}}{m_s} \theta \right) \right], \quad (17)$$

with $\bar{m} \equiv \left(\frac{1}{m_l} + \frac{1}{m_l} + \frac{1}{m_s} \right)^{-1}$. We thus find [19],

$$\begin{aligned} \chi_{\text{top}} &= \bar{m}^2 \left[\frac{\langle \bar{u}u \rangle}{m_l} + \frac{\langle \bar{d}d \rangle}{m_l} + \frac{\langle \bar{s}s \rangle}{m_s} + \chi_P^{uu} + \chi_P^{dd} + \chi_P^{ss} + 2\chi_P^{ud} + 2\chi_P^{us} + 2\chi_P^{ds} \right] \\ &= \frac{1}{4} [m_l (\langle \bar{u}u \rangle + \langle \bar{d}d \rangle) + m_l^2 \chi_\eta] = m_s \langle \bar{s}s \rangle + m_s^2 \chi_P^{ss}. \end{aligned} \quad (18)$$

It is important to note that the topological susceptibility in Eq. (18) vanishes if either of the quarks get massless,

$$\chi_{\text{top}} = 0 \quad (\text{for } m_l \text{ or } m_s = 0), \quad (19)$$

which reflects the flavor singlet nature of the QCD- θ vacuum.

D. Correlation between susceptibility functions

By combining the anomalous Ward-Takahashi identities in Eq. (4) with χ_{top} in Eq. (18), the topological susceptibility can be also rewritten as

$$\chi_{\text{top}} = \frac{1}{4} m_l^2 (\chi_\eta - \chi_\pi). \quad (20)$$

Inserting the scalar-meson susceptibility in Eq. (20), we eventually obtain the crucial formula for understanding the QCD vacuum structure:

$$\begin{aligned} \frac{1}{4} m_l^2 (\chi_{\eta-\delta} - \chi_{\pi-\delta}) &= \chi_{\text{top}}, \\ \frac{1}{4} m_l^2 (\chi_{\eta-\sigma} - \chi_{\pi-\sigma}) &= \chi_{\text{top}}. \end{aligned} \quad (21)$$

Of interest is that the susceptibility functions for the chiral symmetry, the axial symmetry and the topological charge are merged into a single equation. Therefore Eq. (21) is valuable in considering the nontrivial correlation between the symmetry breaking and the topological feature in the susceptibility functions. In particular, it is shown that the difference between the indicator for the chiral symmetry breaking strength $\chi_{\eta-\delta}$ ($\chi_{\pi-\sigma}$) and the indicator for the axial symmetry breaking strength $\chi_{\pi-\delta}$ ($\chi_{\eta-\sigma}$) corresponds to the topological susceptibility.

E. Nontrivial coincidence between chiral and axial symmetry breaking

As shown in the trivial limit of Eq. (9) the strength of the chiral symmetry breaking certainly coincides with that of the axial one due to the absence of the gluonic quantum anomaly in the $U(1)_A$ symmetry. Once we include the quantum corrections in the QCD generating functional, it is inevitable that the $U(1)_A$ anomaly shows up in the axial current. Thus, one might think that there does not exist the limit of the nontrivial coincidence between the chiral and axial symmetry breaking strength in the nonperturbative QCD vacuum. However, paying attention to the flavor singlet nature of the topological susceptibility, we can find a nontrivial coincidence while saving the gluonic $U(1)_A$ anomaly.

From Eq. (21), we note that the discrepancy between the strength of the chiral and axial symmetry breaking in the meson susceptibility functions can be controlled by the topological susceptibility. This implies that the discrepancy can be tuned to be zero by taking the massless limit of the strange quark, due to the flavor singlet nature in Eq. (19):

$$\begin{cases} \chi_{\eta-\delta} = \chi_{\pi-\delta} \\ \chi_{\eta-\sigma} = \chi_{\pi-\sigma} \end{cases}, \quad (\text{for } g \neq 0, m_l \neq 0 \text{ and } m_s = 0). \quad (22)$$

Remarkably, the coincidence between the strength of the chiral and axial symmetry breaking is realized for the QCD vacuum even if the gluonic quantum correction in the $U(1)_A$ anomaly is taken into account. Note that the chiral $SU(2)$ symmetry cannot be seen in the susceptibility functions due to the spontaneous chiral symmetry breaking. At the nontrivial limit in Eq. (22), the quantum $U(1)_A$ anomaly contribution in the associated meson channels is disentangled from the spontaneous-chiral breaking in the meson susceptibility functions.

Once the strange quark obtains a finite mass, the topological susceptibility takes a nonzero value and gives the interference for the correlation between the chiral symmetry breaking in $\chi_{\eta-\delta}$ ($\chi_{\pi-\delta}$) and the axial symmetry breaking in $\chi_{\pi-\delta}$ ($\chi_{\eta-\sigma}$) through Eq. (21). Namely, the coincidence between the chiral and axial symmetry breaking in Eq. (22) is *spoiled* by the finite strange quark mass through nonzero topological susceptibility. This is how in the real-life QCD, the sizable discrepancy between the chiral and axial symmetry breaking emerges due to a sufficiently large current mass of the strange quark controlling the presence of χ_{top} . Intriguingly, given the existence of the nontrivial coincidence in Eq. (22), we may identify the topological susceptibility controlled by the strange quark mass as an indicator for the discrepancy between the chiral and axial symmetry breaking strength in the meson susceptibility functions. Moreover, the nontrivial coincidence in Eq. (22) persists even at finite temperatures. This implies that the chiral symmetry is simultaneously restored with the axial symmetry in hot QCD at the massless limit of the strange quark. The simultaneous symmetry restoration occurs regardless of the order of the chiral phase transition. Thus, Eq. (22) is a key limit to give us a new aspect of the chiral and axial phase transitions in QCD, which would help deepen our understanding of the QCD phase structure.

With those preliminaries, we may now pay attention to the Columbia plot to consider the quark mass dependence on the symmetry restoration. Figure 1 shows the conventional Columbia plot where the QCD phase diagram is described on the $m_{u,d}-m_s$ plane. As a result of Eq. (22), the chiral symmetry is simultaneously restored with the axial symmetry on the $m_{u,d}$ -axis.

In the next section, in order to explain the implication of the nontrivial coincidence in Eq. (22) on the chiral-axial phase diagram, we will investigate the interference of the topological susceptibility for the chiral and axial symmetry breaking based on the NJL model. This will be visualized by drawing the chiral-axial phase diagram in the $m_{u,d}-m_s$ plane, describing the trend of the chiral and axial symmetry restoration.

III. CHIRAL AND AXIAL SYMMETRY BREAKING IN LOW-ENERGY QCD DESCRIPTION

A. Nambu-Jona-Lasinio model

To make the qualitative understanding of the nontrivial correlation among susceptibility functions in Eq. (21) more explicit, we employ an NJL-model analysis, based on the chiral symmetry and the $U(1)_A$ symmetry of the underlying QCD possessions. As will be mentioned later, the NJL model predictions are shown to be in good agreement with the lattice QCD results at finite temperatures. In this subsection, we briefly introduce the NJL model description. Later, we will show the formulae for the susceptibility functions in the framework of the NJL model approach.

The NJL model-Lagrangian with three quark flavors is given as

$$\mathcal{L} = \bar{q}(i\gamma_\mu\partial^\mu - \mathbf{m})q + \mathcal{L}_{4f} + \mathcal{L}_{\text{KMT}}. \quad (23)$$

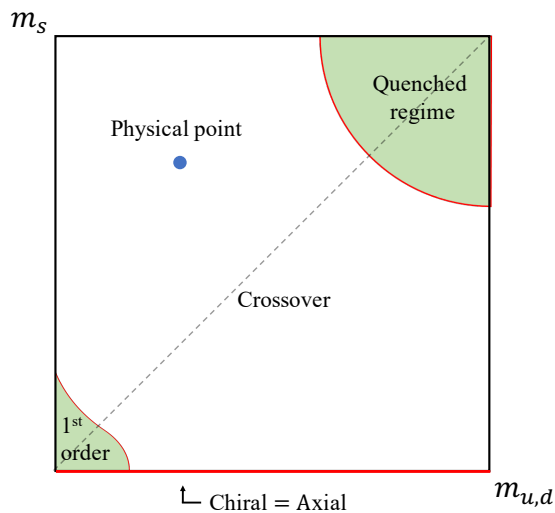


FIG. 1: Conventional Columbia plot. The strength of chiral symmetry breaking coincides with the axial symmetry breaking strength in the meson susceptibility functions with $m_s = 0$ due to the vanishing topological susceptibility. Thus, the simultaneous symmetry restoration between the chiral $SU(2)$ and $U(1)_A$ is realized on the $m_{u,d}$ axis independently of the order of the chiral phase transition.

The four-quark interaction term \mathcal{L}_{4f} is invariant under the chiral $U(3)_L \times U(3)_R$ transformation: $q \rightarrow U \cdot q$ where $U = \exp[-i\gamma_5 \sum_{a=0}^8 (\lambda^a/2)\theta^a]$ with λ_a ($a = 0, 1, \dots, 8$) being the Gell-Mann matrices in the flavor space together with $\lambda_0 = \sqrt{2/3} \cdot 1_{3 \times 3}$ and θ^a the chiral phases. It takes the form

$$\mathcal{L}_{4f} = \frac{g_s}{2} \sum_{a=0}^8 [(\bar{q}\lambda^a q)^2 + (\bar{q}i\gamma_5\lambda^a q)^2], \quad (24)$$

where g_s is the coupling constant.

In the NJL model approach, the anomalous $U(1)_A$ part is described by the determinant form, called the Kobayashi-Maskawa-'t Hooft (KMT) term [26–29],

$$\mathcal{L}_{\text{KMT}} = g_D [\det \bar{q}(1 + \gamma_5)q + \text{h.c.}] \quad (25)$$

with the constant real parameter g_D . Note that the axial breaking \mathcal{L}_{KMT} , which would be induced from the QCD instanton configuration, still keeps the chiral $SU(3)_L \times SU(3)_R$ symmetry.

The current conservation of the chiral symmetry and the $U(1)_A$ symmetry becomes anomalous due to the presence of the quark mass terms and the KMT term:

$$\begin{aligned} \partial_\mu j_A^{a\mu} &= i\bar{q} \left\{ \mathbf{m}, \frac{\tau^a}{2} \right\} \gamma_5 q, \\ \partial_\mu j_A^\mu &= 2i\bar{q}\mathbf{m}\gamma_5 q - 4N_f g_D \text{Im} [\det \bar{q}(1 - \gamma_5)q], \end{aligned} \quad (26)$$

where the curly brackets $\{, \}$ represents an anticommutator. In the spirit of effective models based on the underlying QCD, the anomalous conservation laws of the NJL model have to be linked with those of the underlying QCD, in Eq. (8). Thus, the KMT operator, $g_D \text{Im} [\det \bar{q}(1 - \gamma_5)q]$, may mimic the $U(1)_A$ anomaly of the gluonic operator, $g^2 \epsilon^{\mu\nu\rho\sigma} F_{\mu\nu}^a F_{\rho\sigma}^a$. One should notice here that the $U(1)_A$ anomaly described by the KMT term can vanish by taking $g_D \rightarrow 0$. As far as the $U(1)_A$ anomaly contribution is concerned, this limit corresponds to turning off the QCD gauge coupling g , which is equivalent to the trivial limit for the vanishing axial anomaly ^{#2}.

^{#2} Note that even in the case of the vanishing anomaly associated with $g_D = 0$ the NJL model is still an interacting theory due to the existence of the four-quark interaction term. Although g_D is not completely compatible with the QCD coupling constant g , we can monitor the $U(1)_A$ anomaly contribution through the effective coupling constant g_D .

B. Mean-field approximation and vacuum of NJL model

In this work, we employ the mean-field approximation corresponding to the large N_c expansion. Within the mean-field approximation, the interaction terms go like

$$\begin{aligned}\mathcal{L}_{4f} &\rightarrow 2g_s (\alpha \bar{u}u + \beta \bar{d}d + \gamma \bar{s}s) - g_s(\alpha^2 + \beta^2 + \gamma^2), \\ \mathcal{L}_{\text{KMT}} &\rightarrow 2g_D (\beta\gamma \bar{u}u + \alpha\gamma \bar{d}d + \alpha\beta \bar{s}s) - 4g_D \alpha\beta\gamma,\end{aligned}\quad (27)$$

where α, β , and γ denote the quark condensates,

$$\langle \bar{u}u \rangle \equiv \alpha, \quad \langle \bar{d}d \rangle \equiv \beta, \quad \langle \bar{s}s \rangle \equiv \gamma, \quad (28)$$

In the isospin symmetric limit ($m_u = m_d = m_l$), α and β are taken as $\alpha = \beta$. Hence, the NJL Lagrangian is reduced to the mean-field Lagrangian $\mathcal{L}_{\text{mean}}$:

$$\begin{aligned}\mathcal{L} &= \bar{q}(i\gamma^\mu \partial_\mu - \mathbf{m})q + \frac{g_s}{2} [(\bar{q}\lambda_a q)^2 + (\bar{q}i\gamma_5 \lambda_a q)^2] + g_D \det[\bar{q}(1 + \gamma_5)q + \text{h.c.}] \\ \rightarrow \mathcal{L}_{\text{mean}} &= \bar{q}(i\gamma^\mu \partial_\mu - \mathbf{M})q - g_s(\alpha^2 + \beta^2 + \gamma^2) - 4g_D \alpha\beta\gamma,\end{aligned}\quad (29)$$

where $\mathbf{M} = \text{diag}(M_u, M_d, M_s)$ represents the mass matrix of the dynamical quarks,

$$\begin{aligned}M_u &= m_u - 2g_s \alpha - 2g_D \beta\gamma, \\ M_d &= m_d - 2g_s \beta - 2g_D \alpha\gamma, \\ M_s &= m_s - 2g_s \gamma - 2g_D \alpha\beta.\end{aligned}\quad (30)$$

By integrating out the quark field in the generating functional of the mean-field Lagrangian, the effective potential at finite temperature is evaluated as (see e.g., [30])

$$V_{\text{eff}}(\alpha, \beta, \gamma) = g_s(\alpha^2 + \beta^2 + \gamma^2) + 4g_D \alpha\beta\gamma - 2N_c \sum_i \int^\Lambda \frac{d^3p}{(2\pi)^3} \left\{ E_i + 2T \ln \left(1 + e^{-E_i/T} \right) \right\}, \quad (31)$$

where $N_c = 3$ denotes the number of colors, and $E_i = \sqrt{M_i^2 + p^2}$ are the energies of the constituent quarks. The NJL model is a nonrenormalizable theory. Hence the momentum cutoff Λ should be prescribed in the quark loop calculation to regularize the ultraviolet divergence. In Eq.(31) we have applied a sharp cutoff regularization to the three-dimensional momentum integration.

The quark condensates sit on the stationary point of the effective potential with respect to α, β , and γ , which are determined from the stationary conditions for the effective potential,

$$\frac{\partial V_{\text{eff}}(\alpha, \beta, \gamma)}{\partial \alpha} = 0, \quad \frac{\partial V_{\text{eff}}(\alpha, \beta, \gamma)}{\partial \beta} = 0, \quad \frac{\partial V_{\text{eff}}(\alpha, \beta, \gamma)}{\partial \gamma} = 0. \quad (32)$$

By solving the stationary conditions, one can obtain the following analytic expression of the quark condensates, which corresponds to the quark one-loop result:

$$\langle \bar{q}_i q_i \rangle = -2N_c \int^\Lambda \frac{d^3p}{(2\pi)^3} \frac{M_i}{E_i} [1 - 2(\exp(E_i/T) + 1)^{-1}]. \quad (33)$$

C. Scalar- and pseudoscalar-meson susceptibility in NJL model

In this subsection, we introduce the pseudoscalar meson susceptibilities in the NJL model approach. First, the pseudoscalar susceptibilities, which construct the meson susceptibilities in Eq.(1), are evaluated as [31]

$$\chi_P^{ab}(\omega = 0, \mathbf{p} = 0) = \lim_{p \rightarrow 0} \int_T d^4x e^{ip \cdot x} \langle (i\bar{q}(x)\gamma_5 \lambda^a q(x))(i\bar{q}(0)\gamma_5 \lambda^b q(0)) \rangle, \quad (34)$$

with the external momentum $p^\mu = (\omega, \mathbf{p})$. The susceptibilities are defined by the two-point correlation function of the quark bilinear field at the zero external momentum, $p^\mu = 0$.

We work in the Random Phase Approximation [31], so that the pseudoscalar susceptibilities are evaluated only through the resummed polarization diagram of the quark loop, taking into account the four-point interactions in the NJL model. Within the mean-field approximation, these four-point interaction terms represent fluctuations from the vacuum characterized by the nonzero quark condensates,

$$\begin{aligned}
\mathcal{L}_{\text{fluc}}^{(4)} = & \frac{1}{2} \left(g_s + \frac{2}{3}(\alpha + \beta + \gamma)g_D \right) \bar{q}q\bar{q}q + \frac{1}{2}(g_s - g_D\gamma) \sum_{i=1}^3 \bar{q}\lambda^i q\bar{q}\lambda^i q + \frac{1}{2} \left(g_s + \frac{1}{3}(\gamma - 2\alpha - 2\beta)g_D \right) \bar{q}\lambda^8 q\bar{q}\lambda^8 q \\
& + \left(\frac{\sqrt{2}}{6}(2\gamma - \alpha - \beta)g_D \right) \bar{q}q\bar{q}\lambda^8 q + \left(-\frac{g_D}{\sqrt{6}}(\alpha - \beta) \right) \bar{q}q\bar{q}\lambda_3 q + \left(\frac{g_D}{\sqrt{3}}(\alpha - \beta) \right) \bar{q}\lambda_3 q\bar{q}\lambda_8 q \\
& + \frac{1}{2} \left(g_s - \frac{2}{3}(\alpha + \beta + \gamma)g_D \right) \bar{q}i\gamma_5 q\bar{q}i\gamma_5 q + \frac{1}{2}(g_s + g_D\gamma) \sum_{i=1}^3 \bar{q}i\gamma_5 \lambda^i q\bar{q}i\gamma_5 \lambda^i q \\
& + \frac{1}{2} \left(g_s - \frac{1}{3}(\gamma - 2\alpha - 2\beta)g_D \right) \bar{q}i\gamma_5 \lambda^8 q\bar{q}i\gamma_5 \lambda^8 q \\
& + \left(-\frac{\sqrt{2}}{6}(2\gamma - \alpha - \beta)g_D \right) \bar{q}i\gamma_5 q\bar{q}i\gamma_5 \lambda^8 q + \left(\frac{g_D}{\sqrt{6}}(\alpha - \beta) \right) \bar{q}i\gamma_5 q\bar{q}i\gamma_5 \lambda_3 q + \left(\frac{g_D}{\sqrt{3}}(\alpha - \beta) \right) \bar{q}i\gamma_5 \lambda_3 q\bar{q}i\gamma_5 \lambda_8 q \\
& + \dots
\end{aligned} \tag{35}$$

Here we have picked up only the interaction terms relevant to $\chi_{\pi, \eta, \delta, \sigma}$. Note that since we keep the isospin symmetry, i.e., $\alpha = \beta$, the four-point interaction terms proportional to $(\alpha - \beta)$ vanish, hence those terms will not come into play in the later discussion. Then the pseudoscalar susceptibilities are expressed as

$$\chi_P^{ac} = - \lim_{\omega \rightarrow 0} \lim_{\mathbf{p} \rightarrow 0} \Pi_P^{ab}(\omega, \mathbf{p}) D_{Pbc}^{-1}(\omega, \mathbf{p}), \tag{36}$$

with

$$D_P^{ab}(\omega, \mathbf{p}) = \delta^{ab} + G_P^{ac} \Pi_P^{cb}(\omega, \mathbf{p}), \tag{37}$$

where G_P^{ab} is the coupling strength corresponding to the four-point interaction within the mean field approximation and Π_P^{ab} is the polarization function at the quark one-loop level. Note that χ_P^{ab} , G_P^{ab} and Π_P^{ab} take the matrix form.

The pion susceptibility corresponds to this χ_P^{ab} with $a, b = 1, 2, 3$ as

$$\begin{aligned}
\chi_\pi &= \chi_P^{11} \\
&= - \left[\mathbf{\Pi}_\pi(0, 0) \cdot \left\{ \mathbf{1}_{3 \times 3} + \mathbf{G}_\pi \cdot \mathbf{\Pi}_\pi(\mathbf{0}, \mathbf{0}) \right\}^{-1} \right]^{11} = \chi_P^{22} = \chi_P^{33},
\end{aligned} \tag{38}$$

where the coupling strength in the pion channel $\mathbf{G}_\pi = \text{diag}(G_P^{11}, G_P^{22}, G_P^{33})$ and the pion polarization function $\mathbf{\Pi}_\pi = \text{diag}(\Pi_P^{11}, \Pi_P^{22}, \Pi_P^{33})$ are given as

$$\begin{aligned}
\mathbf{G}_\pi &= (g_s + g_D\gamma) \mathbf{1}_{3 \times 3}, \\
\mathbf{\Pi}_\pi &= (I_P^u + I_P^d) \mathbf{1}_{3 \times 3} = 2I_P^u \mathbf{1}_{3 \times 3},
\end{aligned} \tag{39}$$

with $I_P^i(\omega, \mathbf{p})$ being the pseudoscalar one-loop polarization functions [32],

$$I_P^i(0, 0) = -\frac{N_c}{\pi^2} \int_0^\Lambda dp p^2 \frac{1}{E_i} \left[1 - 2(\exp(E_i/T) + 1)^{-1} \right], \quad \text{for } i = u, d, s. \tag{40}$$

Note that owing to the isospin symmetry, \mathbf{G}_π and $\mathbf{\Pi}_\pi$ exhibit no off-diagonal components. In contrast, as shown in Eq. (35), the flavor symmetry breaking associated with the $U(1)_A$ anomaly provides off-diagonal components in G_P^{ab} and Π_P^{ab} for $a, b = 0, 8$,

$$\mathbf{G}_P = \begin{pmatrix} G_P^{00} & G_P^{08} \\ G_P^{80} & G_P^{88} \end{pmatrix} = \begin{pmatrix} g_s - \frac{2}{3}(\alpha + \beta + \gamma)g_D & -\frac{\sqrt{2}}{6}(2\gamma - \alpha - \beta)g_D \\ -\frac{\sqrt{2}}{6}(2\gamma - \alpha - \beta)g_D & g_s - \frac{1}{3}(\gamma - 2\alpha - 2\beta)g_D \end{pmatrix}, \tag{41}$$

$$\mathbf{\Pi}_P = \begin{pmatrix} \Pi_P^{00} & \Pi_P^{08} \\ \Pi_P^{80} & \Pi_P^{88} \end{pmatrix} = \begin{pmatrix} \frac{2}{3}(2I_P^u + I_P^s) & \frac{2\sqrt{2}}{3}(I_P^u - I_P^s) \\ \frac{2\sqrt{2}}{3}(I_P^u - I_P^s) & \frac{2}{3}(I_P^u + 2I_P^s) \end{pmatrix}. \tag{42}$$

The pseudoscalar susceptibilities in Eq.(5) are obtained as linear combinations of χ_P^{ab} for $a, b = 0, 8$ as

$$\begin{pmatrix} \frac{1}{2}\chi_P^{uu} + \frac{1}{2}\chi_P^{ud} \\ \chi_P^{us} \\ \chi_P^{ss} \end{pmatrix} = \begin{pmatrix} \frac{1}{6} & \frac{\sqrt{2}}{6} & \frac{1}{12} \\ \frac{1}{6} & -\frac{\sqrt{2}}{12} & -\frac{1}{6} \\ \frac{1}{6} & -\frac{\sqrt{2}}{3} & \frac{1}{3} \end{pmatrix} \begin{pmatrix} \chi_P^{00} \\ \chi_P^{08} \\ \chi_P^{88} \end{pmatrix}, \quad (43)$$

where we have taken the isospin symmetric limit into account, i.e., $\chi_P^{uu} = \chi_P^{dd}$ and $\chi_P^{us} = \chi_P^{ds}$. Then the η meson susceptibility is evaluated as

$$\chi_\eta = 2\chi_P^{uu} + 2\chi_P^{ud}. \quad (44)$$

Similarly the scalar meson susceptibilities are given by

$$\chi_S^{ac} = -\Pi_S^{ab}(0, 0)D_{Sbc}^{-1}(0, 0), \quad (45)$$

with

$$D_S^{ab}(0, 0) = \delta^{ab} + G_S^{ac}\Pi_S^{cb}(0, 0) \quad (46)$$

where G_S^{ab} is the coupling strength matrix and Π_S^{ab} is the polarization tensor matrix in the scalar channel.

The explicit formula for χ_δ reads

$$\begin{aligned} \chi_\delta &= \chi_S^{11} \\ &= \left[-\mathbf{\Pi}_\delta(0, 0) \cdot \{\mathbf{1}_{3 \times 3} + \mathbf{G}_\delta \cdot \mathbf{\Pi}_\delta(0, 0)\}^{-1} \right]^{11} = \chi_S^{22} = \chi_S^{33}, \end{aligned} \quad (47)$$

where the coupling strength in the δ meson channel $\mathbf{G}_\delta = \text{diag}(G_S^{11}, G_S^{22}, G_S^{33})$ and the δ -meson polarization function $\mathbf{\Pi}_\delta = \text{diag}(\Pi_S^{11}, \Pi_S^{22}, \Pi_S^{33})$ are given as

$$\begin{aligned} \mathbf{G}_\delta &= (g_s - g_D\gamma)\mathbf{1}_{3 \times 3}, \\ \mathbf{\Pi}_\delta &= (I_S^u + I_S^d)\mathbf{1}_{3 \times 3} = 2I_S^u\mathbf{1}_{3 \times 3}, \end{aligned} \quad (48)$$

with I_S^i being the scalar one-loop polarization functions,

$$I_S^i(0, 0) = -\frac{N_c}{\pi^2} \int_0^\Lambda p^2 dp \frac{E_i^2 - M_i^2}{E_i^3} \{1 - 2[\exp(E_i/T) + 1]^{-1}\}, \quad i = u, d, s. \quad (49)$$

For $a, b = 8$, G_S^{ab} and Π_S^{ab} are given as

$$\mathbf{G}_S = \begin{pmatrix} G_S^{00} & G_S^{08} \\ G_S^{80} & G_S^{88} \end{pmatrix} = \begin{pmatrix} g_s + \frac{2}{3}(\alpha + \beta + \gamma)g_D & \frac{\sqrt{2}}{6}(2\gamma - \alpha - \beta)g_D \\ \frac{\sqrt{2}}{6}(2\gamma - \alpha - \beta)g_D & g_s + \frac{1}{3}(\gamma - 2\alpha - 2\beta)g_D \end{pmatrix} \quad (50)$$

$$\mathbf{\Pi}_S = \begin{pmatrix} \Pi_S^{00} & \Pi_S^{08} \\ \Pi_S^{80} & \Pi_S^{88} \end{pmatrix} = \begin{pmatrix} \frac{2}{3}(2I_S^u + I_S^s) & \frac{2\sqrt{2}}{3}(I_S^u - I_S^s) \\ \frac{2\sqrt{2}}{3}(I_S^u - I_S^s) & \frac{2}{3}(I_S^u + 2I_S^s) \end{pmatrix}. \quad (51)$$

Then, taking the linear combinations of χ_S^{ab} , one can obtain the scalar susceptibilities in Eq. (6),

$$\begin{pmatrix} \frac{1}{2}\chi_S^{uu} + \frac{1}{2}\chi_S^{ud} \\ \chi_S^{us} \\ \chi_S^{ss} \end{pmatrix} = \begin{pmatrix} \frac{1}{6} & \frac{\sqrt{2}}{6} & \frac{1}{12} \\ \frac{1}{6} & -\frac{\sqrt{2}}{12} & -\frac{1}{6} \\ \frac{1}{6} & -\frac{\sqrt{2}}{3} & \frac{1}{3} \end{pmatrix} \begin{pmatrix} \chi_S^{00} \\ \chi_S^{08} \\ \chi_S^{88} \end{pmatrix}, \quad (52)$$

where the isospin symmetric limit has taken into account, $\chi_S^{uu} = \chi_S^{dd}$ and $\chi_S^{us} = \chi_S^{ds}$. From Eq.(52) we obtain the sigma-meson susceptibility χ_σ in the NJL model analysis,

$$\chi_\sigma = 2\chi_S^{uu} + 2\chi_S^{ud}. \quad (53)$$

D. Trivial and nontrivial coincidence of chiral and axial breaking in a view of the NJL description

With Eq. 20 and the pseudscalar meson susceptibility in Eqs. (38) and (44), the topological susceptibility in the NJL model can be described as

$$\chi_{\text{top}} = -m_l m_s g_D \left(\alpha \frac{(\Pi_P^{08})^2 - \Pi_P^{00} \Pi_P^{88}}{6 \det(1 + G_P \Pi_P)} \right). \quad (54)$$

Using Eq. (54) together with the meson susceptibilities in Eqs. (38), (44), (47) and (53), one can easily check that the NJL model reproduces Eq. (21):

$$\begin{aligned} \frac{1}{4} m_l^2 (\chi_{\eta-\delta} - \chi_{\pi-\delta}) &= \chi_{\text{top}}, \\ \frac{1}{4} m_l^2 (\chi_{\eta-\sigma} - \chi_{\pi-\sigma}) &= \chi_{\text{top}}. \end{aligned}$$

Note that the analytical expression of χ_{top} in Eq. (54) explicitly shows that χ_{top} is proportional to the $U(1)_A$ anomaly-related coupling g_D . As was noted, χ_{top} goes away in the limit of the vanishing $U(1)_A$ anomaly, $g_D \rightarrow 0$, while the meson susceptibility functions keep finite values. This is the NJL-model realization of the trivial coincidence between the indicators for the chiral and axial symmetry breaking in the meson susceptibility functions, as in Eq. (9):

$$\begin{cases} \chi_{\eta-\delta} = \chi_{\pi-\delta} \\ \chi_{\eta-\sigma} = \chi_{\pi-\sigma} \end{cases}, \quad (\text{for } g_D = 0, \quad m_l \neq 0 \text{ and } m_s \neq 0). \quad (55)$$

Of crucial is to note also that χ_{top} in Eq. (54) is proportional also to both the light quark mass and the strange quark mass, as the consequence of the flavor singlet nature in Eq. (19). Hence, the NJL model also provides the nontrivial coincidence between the chiral and axial indicators with keeping the $U(1)_A$ anomaly, as derived from the underlying QCD in Eq. (22):

$$\begin{cases} \chi_{\eta-\delta} = \chi_{\pi-\delta} \\ \chi_{\eta-\sigma} = \chi_{\pi-\sigma} \end{cases}, \quad (\text{for } g_D \neq 0, \quad m_l \neq 0 \text{ and } m_s = 0). \quad (56)$$

This coincidence implies that $U(1)_A$ anomaly contribution in the associated meson channels becomes invisible in the meson susceptibility functions at $m_s = 0$ where $\chi_{\text{top}} = 0$, even in the presence of the $U(1)_A$ anomaly ($g_D \neq 0$).

The topological susceptibility has also been studied by some effective model approaches [33–42] However, the previous studies have not taken account of the flavor singlet nature of the topological susceptibility, so that the nontrivial coincidence in Eq.(56) has never been addressed ^{#3}.

IV. QUARK MASS DEPENDENCE ON QCD VACUUM STRUCTURE

In this section, through Eq. (21), we numerically explore the correlations among the susceptibility functions for the chiral symmetry breaking, the axial symmetry breaking and the topological charge.

A. QCD vacuum structure with physical quark masses

To exhibit the numerical results of the susceptibility functions, we take the value of the parameters as listed in Table I [31]. With the input values, the following four hadronic observables are obtained at $T = 0$ [31],

$$m_\pi = 136 \text{ MeV}, \quad f_\pi = 93 \text{ MeV}, \quad m_K = 495.7 \text{ MeV}, \quad m_{\eta'} = 957.5 \text{ MeV}, \quad (57)$$

^{#3} One may further rotate quark fields by the $U(1)_A$ transformation with the rotation angles $\theta_{f=u,d,s}$, so that the NJL Lagrangian is shifted as $\mathcal{L}_{\text{NJL}}(\theta) \rightarrow \mathcal{L}_{\text{NJL}}(\theta - \bar{\theta}) + \bar{\theta} Q_{\text{NJL}}$ where $\bar{\theta} = \theta_u + \theta_d + \theta_s$ and $Q_{\text{NJL}} = -4g_D \text{Im}[\det \bar{q}_i(1 - \gamma_5)q_j]$. By taking the $\bar{\theta} = \theta$, the θ -dependence is completely rotated away from the quark mass term, and then moves to the Q_{NJL} term: $\mathcal{L}_{\text{NJL}}(\theta = 0) + \theta Q_{\text{NJL}}$. Indeed, the topological susceptibility has been evaluated based on the NJL Lagrangian including the θQ_{NJL} term: $\chi_{\text{top}} = \int_T d^4x \langle Q_{\text{NJL}}(x) Q_{\text{NJL}}(0) \rangle$ [33]. However, the θ -dependence on the θQ_{NJL} term accidentally goes away within the ordinary mean-field approach. This is because Q_{NJL} vanishes under the mean-field approximation, $Q_{\text{NJL}} \propto \det[\bar{q}(1 + \gamma_5)q] - \det[\bar{q}(1 - \gamma_5)q] \rightarrow (\beta\gamma\bar{u}u + \alpha\gamma\bar{d}d + \alpha\beta\bar{s}s - 2\alpha\beta\gamma) - (\beta\gamma\bar{u}u + \alpha\gamma\bar{d}d + \alpha\beta\bar{s}s - 2\alpha\beta\gamma) = 0$. Hence, the topological susceptibility can not be evaluated based on $\mathcal{L}_{\text{NJL}}(\theta = 0) + \theta Q_{\text{NJL}}$ within the mean-field approach through the second derivative of the generating functional with respect to θ . Thereby, we do not take this way, instead, directly apply the Eq. (18) which is evaluated from the θ -dependent quark-mass term with the flavor singlet nature.

which are in good agreement with the experimental values. Furthermore, the topological susceptibility at the vacuum ($T = 0$) qualitatively agrees with the lattice observations [43, 44], as discussed in [23].

TABLE I: Parameter setting

parameters	values
light quark mass m_l	5.5 MeV
strange quark mass m_s	138 MeV
four-fermion coupling constant g_s	0.358 fm ²
six-fermion coupling constant g_D	- 0.0275 fm ⁵
cutoff Λ	631.4 MeV

We will not consider intrinsic-temperature dependent couplings, instead, all the T dependence should be induced only from the thermal quark loop corrections. Actually, the present NJL shows good agreement with lattice QCD results on the temperature scaling for the chiral, axial, and topological susceptibilities, as shown in Ref. [23]. In this sense, we do not need to introduce such an intrinsic T dependence for the model parameters in the regime up to temperatures around the chiral crossover.

In Fig. 2, we first show plots of the susceptibilities as a function of temperature. This figure shows that the meson susceptibilities forming the chiral partners (chiral indicators), $\chi_{\eta-\delta}$ and $\chi_{\pi-\sigma}$, smoothly approach zero at high temperatures, but do not exactly reach zero. This tendency implies that the NJL model undergoes a chiral crossover #4.

The pseudocritical temperature of the chiral crossover can be evaluated from the inflection point of $\chi_{\eta-\delta}$ or $\chi_{\pi-\sigma}$ with respect to temperature, $d^2\chi_{\eta-\delta,\pi-\sigma}/dT^2|_{T=T_{pc}} = 0$, and then we find $T_{pc}|_{\text{NJL}} \simeq 189$ MeV. This inflection point coincides with that estimated from the light quark condensate [23]. However the NJL's estimate of the pseudocritical temperature is somewhat bigger than the lattice QCD's, $T_{pc}|_{\text{lat.}} \sim 155$ MeV [10, 46, 47]. In fact, the NJL analysis is implemented in the mean field approximation corresponding to the large N_c limit. The corrections of the beyond mean field approximation would be subject to the size of the next-to-leading order corrections of the large N_c expansion, $O(1/N_c) \sim O(0.3)$. Including the possible corrections to the current model analysis, the NJL's result might be consistent with the lattice observation. Supposing this systematic deviation by about 30% to be accepted within the framework of the the large N_c expansion, one may say that the NJL description at finite temperatures yields qualitatively good agreement with the lattice QCD simulations. Indeed, all the temperature dependence of $\chi_{\eta-\delta}$, $\chi_{\pi-\delta}$, and χ_{top} qualitatively accords with the lattice data [9, 10, 43, 44, 48] (for the detailed discussion, see [23]).

From the panel (a) of Fig. 2, one can see a sizable difference in the meson susceptibilities between the chiral indicator $\chi_{\eta-\delta}$ and the axial indicator $\chi_{\pi-\delta}$ in the low temperature regime: $\chi_{\eta-\delta} \ll \chi_{\pi-\delta}$ for $T < T_{pc}$. A large discrepancy also shows up in the other combination between $\chi_{\pi-\sigma}$ and $\chi_{\eta-\sigma}$: $\chi_{\eta-\sigma} \ll \chi_{\pi-\sigma}$ for $T < T_{pc}$. Looking at the high temperature regime $T > T_{pc}$, one finds that the sizable difference is still kept, $\chi_{\eta-\delta} \ll \chi_{\pi-\delta}$, while $\chi_{\pi-\delta}$ and $\chi_{\eta-\delta}$ get close to zero, as shown in the panel (b) of Fig. 2. This tendency is actually consistent with the lattice QCD observation [9, 10]. In addition, we also find that $\chi_{\sigma-\eta}$ becomes larger than $\chi_{\pi-\sigma}$ at around T_{pc} . As the temperature further increases, $\chi_{\pi-\sigma}$ and $\chi_{\eta-\sigma}$ also approach zero with keeping $|\chi_{\pi-\sigma}| \ll |\chi_{\eta-\sigma}|$ for $T > 1.5T_{pc}$. These trends imply that the chiral symmetry is restored faster than the the $U(1)_A$ symmetry in the meson susceptibility functions at the physical value of the current quark masses.

Hereafter, we will vary the current quark masses while keeping the input values of the coupling constants g_s , g_D , and the cutoff Λ , and will investigate the correlations among the susceptibility functions through Eq. (21) as well as the nontrivial coincidence in Eq. (22). Actually in the present NJL model, as the current quark masses decrease, the chiral crossover is changed to the chiral second order phase transition at $m_\pi^c \simeq 60$ MeV (corresponding to $m_l = m_s = 1.05$ MeV). Thus the chiral-first order-phase transition domain appears for $m_\pi < 60$ MeV. In the next subsequent subsections, we will focus on the chiral crossover and the first order phase transition domains, separately.

#4 What we work on are the susceptibilities, which correspond to meson-correlation functions at zero momentum transfer. This is in contrast to the conventional meson correlators depending on the transfer momentum, from which meson masses are read off. Furthermore, the susceptibilities involve contact term contributions independent of momenta, which could be sensitive to a high-energy scale physics, while the conventional meson correlators are dominated by the low-lying meson mass scale. Nevertheless, the degeneracy of the chiral or axial partners at high temperatures, similar to those detected in the susceptibility, can also be seen in the mass difference or equivalently the degeneracy of the conventional meson correlators for the partners, which is simply because the mass difference plays an alternative indicator of the chiral or axial breaking as observed in the lattice simulation [45].

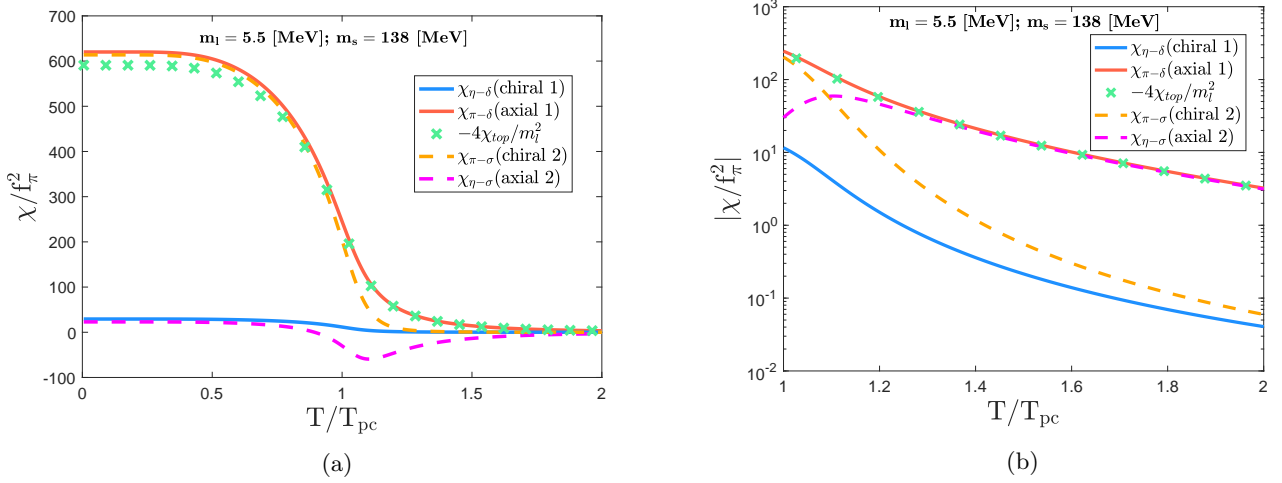


FIG. 2: The temperature dependence of the susceptibility functions at the physical point ($m_l = 5.5$ MeV and $m_s = 138$ MeV) for (a) $T/T_{pc} = 0 - 2$ and (b) $T/T_{pc} = 1 - 2$. The pseudocritical temperature for the chiral crossover has been observed to be $T_{pc} \simeq 189$ MeV. The susceptibility functions have been normalized by square of the pion decay constant ($\simeq 93$ MeV), and the temperature axis also by T_{pc} , so that all quantities are dimensionless to reduce the systematic uncertainty (approximately about 30%) associated with the present NJL model description of QCD. See also the text.

B. Crossover domain

In this subsection, we evaluate the strange quark mass dependence on the susceptibility functions in the crossover domain. We allow the strange quark mass to be off the physical value, while the light quark mass is fixed at the physical one, $m_l = 5.5$ MeV. The present NJL model with this setup exhibits the crossover for the chiral phase transition.

In Fig. 3, we plot the susceptibility functions in the massless limit of the strange quark mass ($m_s = 0$). This figure shows that the topological susceptibility χ_{top} vanishes for any temperature. This must be so due to the flavor singlet nature in Eq. (19). As the consequence of the vanishing χ_{top} , the axial indicator $\chi_{\pi-\delta}$ ($\chi_{\eta-\sigma}$) coincides with the chiral indicator $\chi_{\eta-\delta}$ ($\chi_{\pi-\sigma}$) for the whole temperature regime, so that the chiral $SU(2)_L \times SU(2)_R$ symmetry is simultaneously restored with the $U(1)_A$ symmetry.

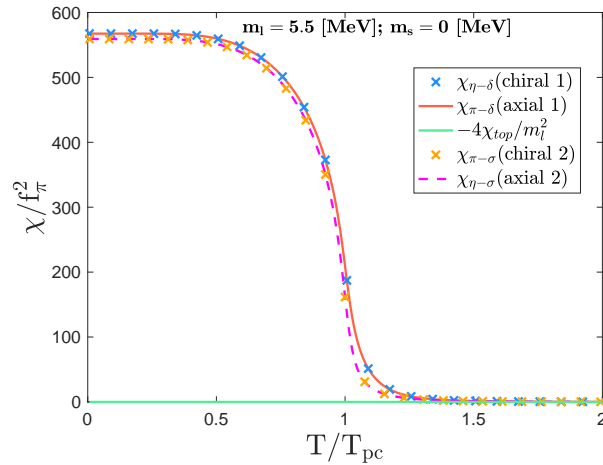


FIG. 3: The plot showing the nontrivial coincidence between the chiral and axial indicators (of two types) in the crossover domain with the massless strange quark ($m_l = 5.5$ MeV and $m_s = 0$; $T_{pc} \simeq 144$ MeV). The topological susceptibility is exactly zero for all temperatures due to the flavor singlet nature associated with the massless strange quark. The scaled factors have been applied on both horizontal and vertical axes in the same way as in Fig. 2.

Once a finite strange quark mass is turned on, the topological susceptibility χ_{top} becomes finite, no matter how m_s is small, as seen in Fig. 4. It is interesting to note that when $m_s \ll m_l$, like in Fig. 4 with $m_s = 10^{-3}m_l$, the topological susceptibility ($-4\chi_{\text{top}}/m_l^2$) is much smaller than the chiral indicator $\chi_{\eta-\delta}$ ($\chi_{\pi-\sigma}$) and the axial indicator $\chi_{\pi-\delta}$ ($\chi_{\eta-\sigma}$). This is because χ_{top} is proportional to the m_s , as the consequence of the flavor singlet nature in Eq. (19). According to the correlation among susceptibility functions in Eq. (21), the chiral indicator $\chi_{\eta-\delta}$ ($\chi_{\pi-\sigma}$) takes almost the same trajectory of what the axial indicator $\chi_{\pi-\delta}$ ($\chi_{\eta-\sigma}$) follows at finite temperatures. Thus, it is the negligible χ_{top} that triggers the (almost) simultaneous symmetry restoration for the chiral and axial symmetries in the case of the tiny strange quark mass, $m_s \ll m_l$.

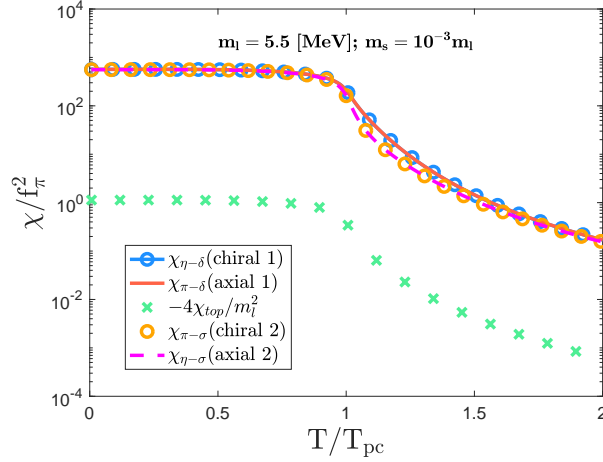


FIG. 4: The plot showing the finiteness of the topological susceptibility along with the temperature dependence of the chiral and axial indicators in the crossover domain with a small strange quark mass ($m_l = 5.5$ MeV and $m_s = 10^{-3}m_l$; $T_{\text{pc}} \simeq 144$ MeV). The same scaling for two axes has been made as in Fig. 2.

As m_s gets greater, the topological susceptibility further grows and χ_{top} starts to significantly contribute to the chiral and axial indicators following the correlation form in Eq. (21). Actually, when the strange quark mass takes of $O(10m_l)$, the topological susceptibility ($-4\chi_{\text{top}}/m_l^2$) becomes on the same order of magnitude of $\chi_{\eta-\delta}$ and $\chi_{\pi-\sigma}$ in the low temperature regime: $-4\chi_{\text{top}}/m_l^2 \sim \chi_{\eta-\delta} \sim \chi_{\pi-\sigma}$ for $T < T_{\text{pc}}$. This trend is depicted in the panel (a) of Fig. 5 for $m_s = 10m_l$. Thus, the sizable discrepancy between the chiral indicator $\chi_{\eta-\delta}$ ($\chi_{\pi-\sigma}$) and the axial indicator $\chi_{\pi-\delta}$ ($\chi_{\eta-\sigma}$) emerges for $T < T_{\text{pc}}$ due to the interference of χ_{top} . As the temperature further increases, the susceptibilities go to zero. However a sizable discrepancy still appear between the chiral and axial indicators: $|\chi_{\eta-\delta}| \ll |\chi_{\pi-\delta}|$ and $|\chi_{\pi-\sigma}| \ll |\chi_{\eta-\sigma}|$ for $T > 1.5T_{\text{pc}}$, as depicted in the panel (b) of Fig. 5. This indicates that the large strange quark mass providing the significant interference of the topological susceptibility urges the faster restoration of the chiral symmetry for $m_s = O(10m_l)$.

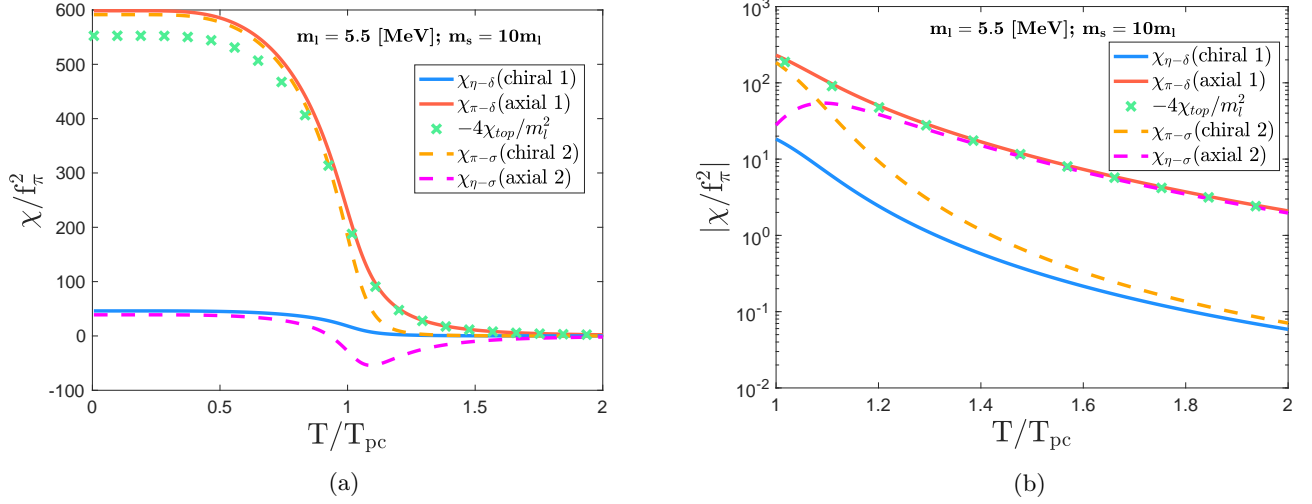


FIG. 5: The plots clarifying the significant interference of the topological susceptibility to make the sizable discrepancy between the chiral and axial indicators in the crossover domain with the large strange quark mass ($m_l = 5.5$ MeV and $m_s = 10m_l$; $T_{pc} \simeq 174$ MeV) for (a) $T/T_{pc} = 0 - 2$ and (b) $T/T_{pc} = 1 - 2$. The manner of scaling axes is the same as in Fig. 2.

C. First order domain

We next consider the first-order phase-transition domain. In this subsection, we fix the light quark mass as $m_l = 0.1$ MeV, and vary the strange quark mass m_s . This setup leads to the first order phase transition for the chiral symmetry.

First of all, see Fig. 6, which shows the susceptibility functions for $m_s = 0$. One can find a jump in meson susceptibility functions at the critical temperature $T_c \simeq 119$ MeV. This jump indicates that the chiral-first order phase transition occurs in the NJL model. Note that even for $T > T_c$ the meson susceptibility functions take finite values due to the presence of the finite light-quark mass, as shown in the panel (b) of Fig. 6. This implies that the chiral and axial symmetries are not completely restored. However, the topological susceptibility is exactly zero because of $m_s = 0$, reflecting the flavor singlet nature of χ_{top} . This is why we observe $\chi_{\eta-\delta} = \chi_{\pi-\delta}$ and $\chi_{\pi-\sigma} = \chi_{\eta-\sigma}$ for the whole temperature (see Fig. 6). In particular, the panel (b) of Fig. 6 shows that $\chi_{\eta-\delta}$ ($\chi_{\pi-\sigma}$) asymptotically goes to zero along with $\chi_{\pi-\delta}$ ($\chi_{\eta-\sigma}$) as the temperature increases. Thus, the chiral symmetry tends to simultaneously restore with the axial symmetry even in the chiral-first order phase-transition domain.

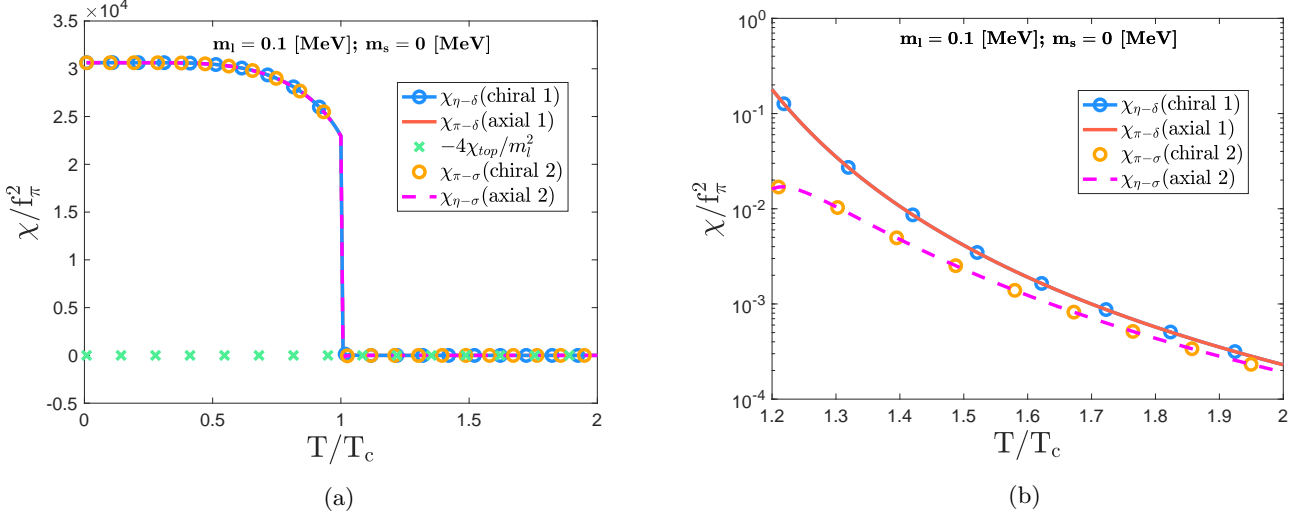


FIG. 6: The plots clarifying the trend of the nontrivial simultaneous restoration for the chiral and axial symmetries even in the chiral-first order phase-transition domain with $m_l = 0.1$ MeV and $m_s = 0$. The panel (a) shows a jump in the mesons susceptibility functions at around $T_c \simeq 119$ MeV, as a consequence of the first order phase transition. The panel (b) closes up the temperature dependence for the chiral and axial indicators after the chiral phase transition. The manner of scaling axes is the same as in Fig. 2. The trend induced by interference of χ_{top} is similar to the one observed in the crossover domain, in Fig. 3.

Next, we supply a finite value for the strange quark mass, to see that the non-vanishing χ_{top} certainly emerges in the first-order phase-transition domain, as in the case of the chiral crossover domain. See Fig. 7. As long as the strange quark mass is small enough, like $m_s \ll m_l$, the topological susceptibility is negligible compared with the chiral and axial indicators. Therefore, the coincidence between the chiral and axial symmetry restoration is effectively almost intact.

As the strange quark mass further increases, the topological susceptibility develops to be non-negligible. For $m_s = \mathcal{O}(10m_l)$, the topological susceptibility ($-4\chi_{\text{top}}/m_l^2$) significantly interferes with the chiral and axial indicators via Eq. (21) and becomes comparable to $\chi_{\pi-\delta}$ and $\chi_{\pi-\sigma}$ for $T < T_c$ (see Fig. 8). For $T > T_c$, we observe a large discrepancy: $|\chi_{\eta-\delta}| \ll |\chi_{\pi-\delta}|$ and $|\chi_{\pi-\sigma}| \ll |\chi_{\eta-\sigma}|$, due to the significant contribution of the topological susceptibility. Thus, the sizable strange quark mass makes the chiral restoration faster than the axial restoration through the non-negligible contribution of the topological susceptibility. Indeed, these trends of the strange quark mass controlling χ_{top} in the first-order phase-transition domain are similar to those observed in the chiral crossover domain.

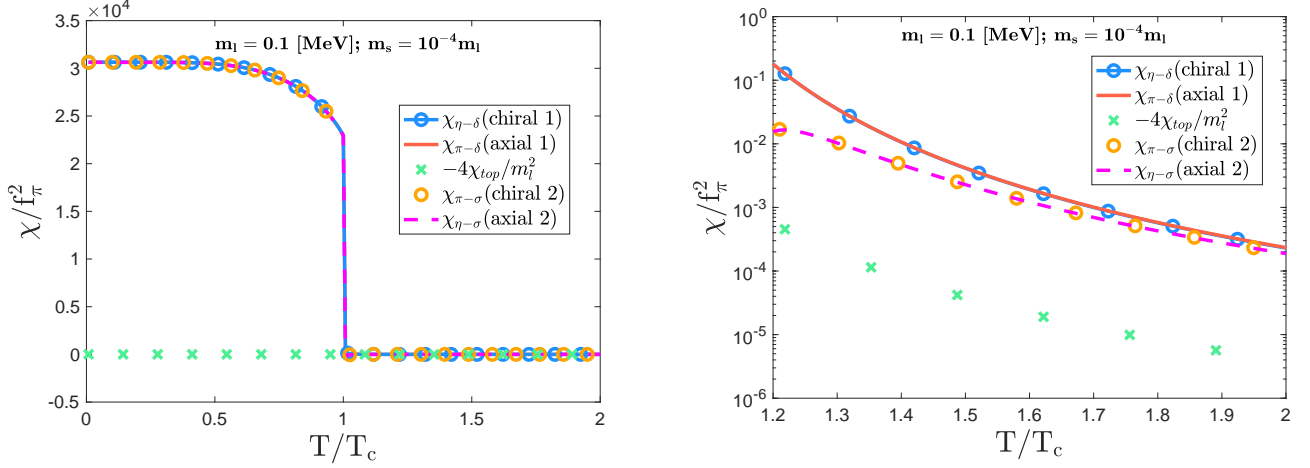


FIG. 7: The plots showing still almost coincidence of the chiral and axial indicators for all temperature ranges, even in the first-order phase-transition domain with $m_l = 0.1$ MeV and $m_s = 10^{-4} m_l$; $T_c \simeq 119$ MeV. The displayed two axes have been scaled in the same way as explained in the caption of Fig. 2. The trend induced by interference of χ_{top} is similar to the one observed in the crossover domain, in Fig. 4.

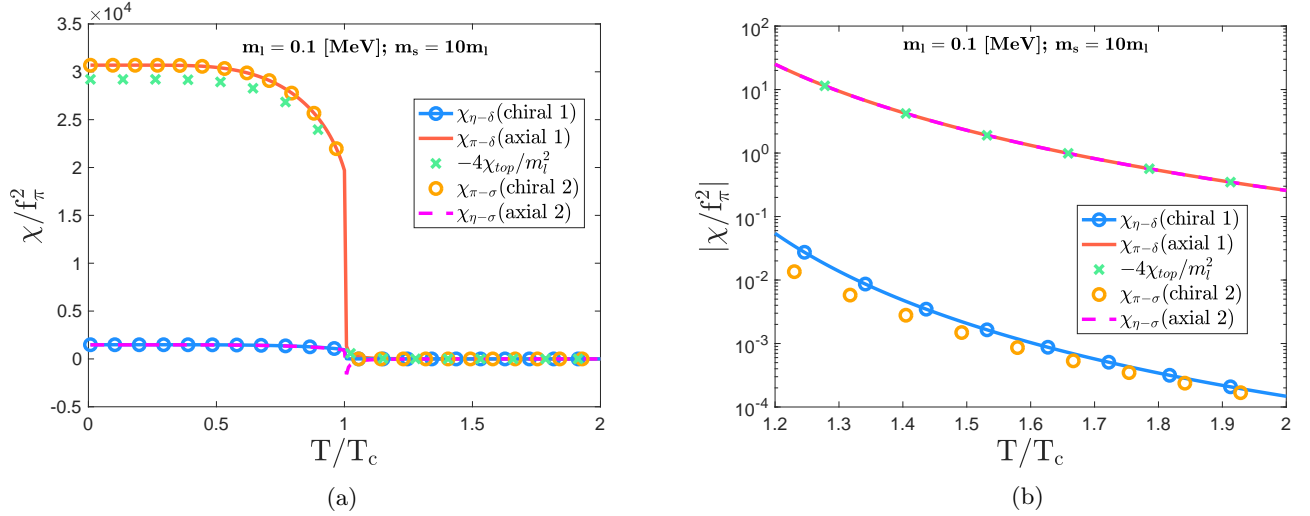


FIG. 8: The plots clarifying the significant interference of χ_{top} with the chiral and axial indicators in the first-order phase-transition domain with $m_l = 0.1$ MeV and $m_s = 10 m_l$; $T_c \simeq 126$ MeV. The displayed two axes have been scaled in the same way as explained in the caption of Fig. 2. The trend induced by interference of χ_{top} is similar to the one observed in the crossover domain, in Fig. 5.

D. Chiral and axial symmetry restorations in view of chiral-axial phase diagram

In the previous subsections, it has been found that the topological susceptibility handled by the strange quark mass is closely related to the meson susceptibilities and interferes with the strengths of the chiral and axial symmetry breaking. Here, we clarify more on the strange quark mass dependence on the restoration trends of the chiral and axial symmetry.

In Fig. 9, we plot the strange quark mass dependence on the difference between the two indicators, $|\chi_{\pi-\delta}| - |\chi_{\eta-\delta}|$ and $|\chi_{\eta-\sigma}| - |\chi_{\pi-\sigma}|$, above the (pseudo)critical temperature $T_{(p)c}$. In particular, $|\chi_{\pi-\delta}| = |\chi_{\eta-\delta}|$ and $|\chi_{\eta-\sigma}| = |\chi_{\pi-\sigma}|$ are realized at $m_s = 0$ even after reaching a high temperature regime where $T \sim (1.5 - 2.5) T_{(p)c}$. This implies that in the case of the massless strange quark, the simultaneous restoration for the chiral and axial symmetries takes place in both the chiral crossover and first order phase transition domains. Once the strange quark obtains a finite mass,

the axial indicator $|\chi_{\pi-\delta}|$ ($|\chi_{\eta-\sigma}|$) starts to deviate from the chiral indicator $|\chi_{\eta-\delta}|$ ($|\chi_{\pi-\sigma}|$) due to the emergence of nonzero χ_{top} . Actually, Fig. 9 shows that the strength of the axial symmetry breaking in the meson susceptibilities is enhanced by the finite strange quark mass through the interference of the topological susceptibility. Furthermore, the discrepancy between the axial indicator $|\chi_{\pi-\delta}|$ ($|\chi_{\eta-\sigma}|$) and the chiral indicator $|\chi_{\eta-\delta}|$ ($|\chi_{\pi-\sigma}|$) persists even at the high temperature $T \sim 2.5 T_{\text{pc}}$. Therefore the axial restoration tends to be delayed, later than the chiral restoration as the strange quark mass gets heavier.

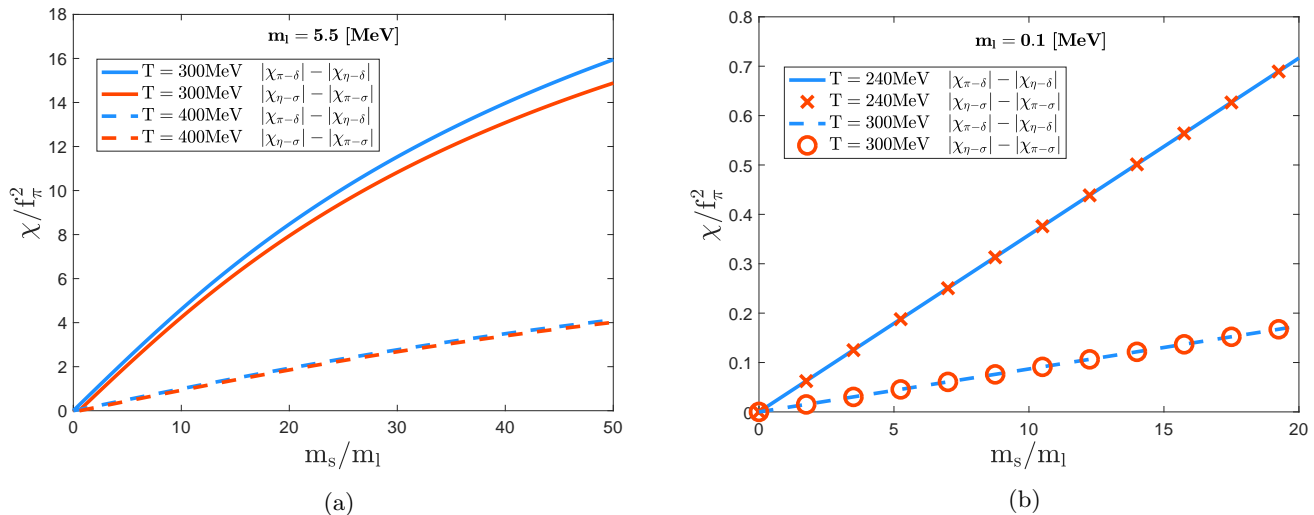


FIG. 9: The strange quark mass dependence on the difference between the axial indicator $|\chi_{\pi-\delta}|$ ($|\chi_{\eta-\sigma}|$) and the chiral indicator $|\chi_{\eta-\delta}|$ ($|\chi_{\pi-\sigma}|$) in (a) the crossover domain and (b) the first-order phase-transition domain. In the crossover domain with $m_s/m_l = 0$ (50), the pseudocritical temperature is evaluated as $T_{\text{pc}} \simeq 144$ (200) MeV, and then the temperatures $T = 300 - 400$ MeV displayed as in panel (a) correspond to $T \simeq (1.5 - 2.8) T_{\text{pc}}$. On the other hand, in the first-order phase-transition domain, the temperatures $T = 240 - 300$ MeV as fixed in panel (b) correspond to $T \simeq (1.8 - 2.5) T_c$, where $T_c \simeq 119$ (130) MeV for $m_s/m_l = 0$ (20).

Finally, we draw the predicted tendency of the chiral and axial restorations in a chiral-axial phase diagram on the $m_{u,d}-m_s$ plane, which is shown in Fig. 10. This phase diagram is a sort of the Columbia plot, in which we reflect the discrepancy between the chiral and axial restorations in terms of the meson susceptibilities at around $T \sim (1.5 - 2.0) T_{\text{pc}}$.

V. SUMMARY AND DISCUSSION

The anomalous chiral-Ward identity in Eq. (20) relating the topological susceptibility to the pseudoscalar meson susceptibility functions has been often used to measure the effective restoration of the $U(1)$ axial symmetry in the $SU(2)$ chiral symmetric phase so far. The $U(1)_A$ restoration probed by the topological susceptibility has extensively been studied in the chiral effective model approaches [33–42] and the lattice QCD frameworks [9, 10, 43, 44, 48] to explore the origin of the split in restorations of the chiral $SU(2)$ symmetry and the $U(1)$ axial symmetry. This ordinary method is summarized in the panel (a) of Fig. 11). However, this ordinary approach suffers from practical difficulty in accessing the origin of the split without ambiguity, because the chiral $SU(2)$ symmetry breaking is highly contaminated with the $U(1)$ axial symmetry breaking even at the beginning, at the vacuum.

In this paper, we have found a new approach: it is the strange quark mass that controls the strengths of the chiral $SU(2)$ symmetry breaking and the $U(1)$ axial symmetry breaking, and those strengths coincide in the limit $m_s = 0$. The idea is to depart from a nontrivial coincidence limit emerging even in the presence of nonzero $U(1)_A$ anomaly due to the nonperturbatively interacting QCD, in sharp contrast to the trivial equivalence between the chiral and axial breaking, where QCD gets reduced to the free quark theory. Of course, the nontrivial coincidence is robust because it is tied with the anomalous chiral Ward-Takahashi identity, Eq. (21), and the flavor-singlet condition of the topological susceptibility. Hence it holds even at finite temperatures, so that the chiral symmetry is simultaneously restored with the axial symmetry regardless of the order of the chiral phase transition. The simultaneous restoration at $m_s = 0$ is viewed as a significant limit to consider the symmetry restorations on the quark mass plane. Given the ‘‘rigid’’ limit of $m_s \rightarrow 0$, we can unambiguously understand that the split in the restorations of the chiral $SU(2)$ and

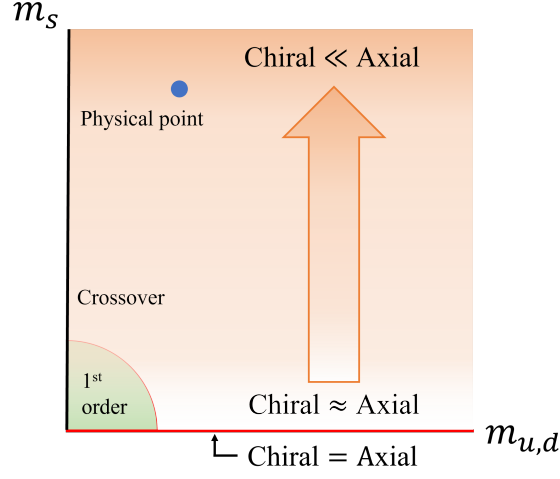


FIG. 10: The predicted chiral-axial phase diagram on the $m_{u,d}$ - m_s plane, in which the discrepancy of the chiral and axial symmetry restorations at around $T \sim (1.5 - 2.0)T_{(p)c}$ is drawn by the shaded area. When the strength of the axial symmetry breaking deviates from the chiral breaking strength to be large, the shaded areas become thick. The nontrivial coincidence as in Eq. (22), is associated with the vanishing χ_{top} , which is located on the $m_{u,d}$ axis. When the strange quark mass gets a finite mass, the axial restoration deviates from the chiral restoration. At around $m_l = O(10m_l)$, the axial restoration is much later than the chiral restoration due to the significant interference of χ_{top} . Namely, at the physical quark masses, the topological susceptibility provides the large discrepancy between the chiral and axial restorations in the meson susceptibilities.

$U(1)_A$ is handled by the strange quark mass ($m_s \neq 0$). This new point of view for symmetry restorations is described in the panel (b) of Fig. 11.

To be concrete, we have employed the NJL model with three flavors to monitor the essential chiral and axial features that QCD possesses. We have confirmed that the NJL model surely provides the nontrivial coincidence of the chiral and axial breaking in the case of $m_s = 0$ in terms of the meson susceptibility functions, and exhibits the simultaneous restoration for the chiral and axial symmetries in both the chiral crossover and the first-order phase-transition cases:

$$\begin{cases} \chi_{\eta-\delta} = \chi_{\pi-\delta} \rightarrow 0 \\ \chi_{\eta-\sigma} = \chi_{\pi-\sigma} \rightarrow 0 \end{cases}, \quad (\text{for } T > T_{(p)c}, \quad g_D \neq 0, \quad m_l \neq 0 \text{ and } m_s = 0). \quad (58)$$

Once the strange quark gets massive, the topological susceptibility takes a finite value and interferes with the meson susceptibility functions through Eq. (21). The simultaneous restoration for the chiral and axial symmetries is controlled by the strange quark mass through the interference of nonzero χ_{top} . Thus, with the large strange quark mass ($m_s \gg m_l$), the chiral restoration significantly deviates from the axial restoration above the (pseudo)critical temperature:

$$\begin{cases} \chi_{\eta-\delta} \rightarrow 0, \quad \chi_{\pi-\delta} \rightarrow 0 \quad \text{with} \quad |\chi_{\pi-\delta}| \gg |\chi_{\eta-\delta}| \\ \chi_{\eta-\sigma} \rightarrow 0, \quad \chi_{\pi-\sigma} \rightarrow 0 \quad \text{with} \quad |\chi_{\eta-\sigma}| \gg |\chi_{\pi-\sigma}| \end{cases}, \quad (\text{for } T > 1.5T_{(p)c}, \quad g_D \neq 0, \quad m_l \neq 0 \text{ and } m_s \neq 0). \quad (59)$$

Due to the significant interference of the topological susceptibility, the chiral symmetry is restored faster than the axial symmetry in the $2 + 1$ flavor case with the physical quark masses. Figure 10 shows a schematic view of the evolution of the chiral and axial breaking deviating from the nontrivial coincidence limit toward real-life QCD.

In closing the present paper, we give a list of several comments on our findings and another intriguing aspect of the nontrivial coincidence between the chiral and axial symmetry breaking strengths.

- The predicted chiral-axial phase diagram in Fig. 10 is a new guideline for exploring the influence of the $U(1)_A$ anomaly on the chiral phase transition, which is sort of giving a new interpretation of the conventional Columbia plot. Further studies are desired in lattice QCD simulations to draw definitely conclusive benchmarks on the chiral-axial phase diagram.
- The existence of the nontrivial coincidence implies that the $U(1)_A$ anomaly can be controlled by the current mass of the strange quark. The controllable anomaly could give a new understanding of the η' meson mass originated from the $U(1)_A$ anomaly. The investigation for the m_s -dependence on the pseudoscalar meson masses would thus be a valuable study.

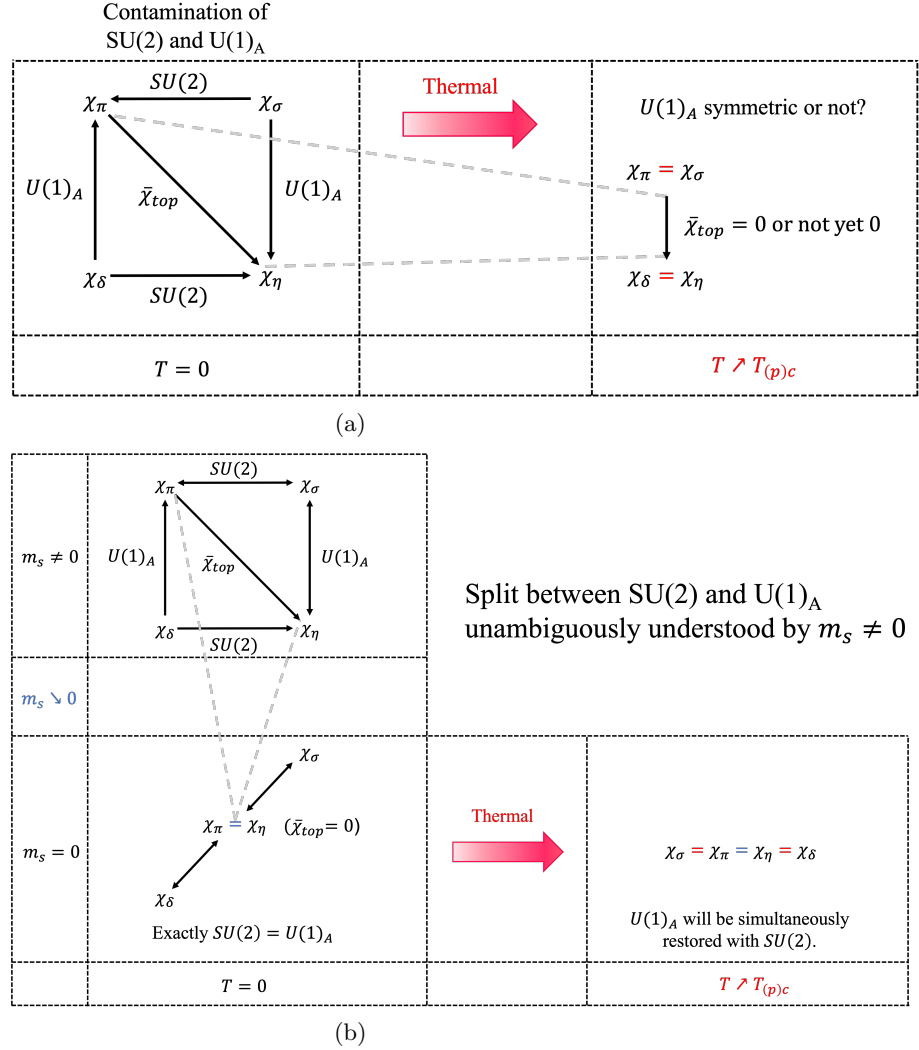


FIG. 11: The split in the restorations of the chiral $SU(2)$ symmetry and the $U(1)$ axial symmetry at hot QCD. (a): ordinary way to address the symmetry restorations. The ambiguous origin of the effective $U(1)_A$ restoration is often measured by the topological susceptibility (which is normalized by the quark mass, $\bar{\chi}_{top} = 4\chi_{top}/m_l^2$). (b): new point of view for symmetry restorations at $m_s = 0$. Due to the anomalous Ward-Takahashi identity at hot QCD, the chiral $SU(2)$ symmetry breaking exactly coincides with the $U(1)_A$ symmetry breaking, and this coincidence holds for any temperatures. As a robust consequence, when the chiral $SU(2)$ symmetry is restored at the (pseudo)critical temperature, the $U(1)_A$ symmetry is simultaneously restored. Therefore, the limit $m_s = 0$ manifests the symmetry restorations on the quark mass plane: it can be unambiguously understood that the strange quark mass handles the split in the restorations of chiral $SU(2)$ symmetry and the $U(1)_A$ symmetry at hot QCD with the three quark flavors having finite masses.

- The fate of the $U(1)_A$ anomaly in the nuclear/quark matter is a longstanding problem and has attracted people a lot so far. The nontrivial coincidence should also be realized in the finite dense matter involving the massless strange quark. The nontrivial coincidence at finite density might shed light on a novel insight for the partial $U(1)_A$ restoration in the medium with physical quark masses.
- The contribution of the $U(1)_A$ anomaly to the color confinement is an open question. It would be worth including the Polyakov loop terms in the NJL model to address the correlation between the nontrivial coincidence of the chiral and axial breaking and the deconfinement-confinement phase transition.
- Though the NJL model produces the qualitative results consistent with lattice observations, it would be a rough analysis due to the mean field approximation. However, the existence of the nontrivial coincidence is robust because it is based on the anomalous Ward identity, This should thus be seen even beyond the mean field approximation that the present NJL study has assumed, or even more rigorous nonperturbative analyses such

as those based on the lattice NJL-model and the functional renormalization group method.

- The nontrivial chiral-axial coincidence is generic phenomenon, which can also be seen in a generic class of QCD-like theories with “1 ($m_s = 0$)+ 2 (m_l) flavors”, involving models beyond the standard model. In particular, the coincidence in the first-order phase transition case might impact on cosmological implications of QCD-like scenarios with axionlike particles associated with the axial breaking, including the gravitational wave probes. Investigation along also this line might be interesting.

Acknowledgements

We are grateful to Hen-Tong Ding for useful comments. This work was supported in part by the National Science Foundation of China (NSFC) under Grant No.11975108, 12047569, 12147217 and the Seeds Funding of Jilin University (S.M.). The work of A.T. was supported by the RIKEN Special Postdoctoral Researcher program and partially by JSPS KAKENHI Grant Number JP20K14479. M.K. was supported by the Fundamental Research Funds for the Central Universities and partially by the National Natural Science Foundation of China (NSFC) Grant Nos: 12235016, and the Strategic Priority Research Program of Chinese Academy of Sciences under Grant No XDB34030000.

-
- [1] Robert D. Pisarski and Frank Wilczek. Remarks on the Chiral Phase Transition in Chromodynamics. *Phys. Rev. D*, 29:338–341, 1984.
- [2] S. Ejiri, F. Karsch, E. Laermann, C. Miao, S. Mukherjee, P. Petreczky, C. Schmidt, W. Soeldner, and W. Unger. On the magnetic equation of state in (2+1)-flavor QCD. *Phys. Rev. D*, 80:094505, 2009.
- [3] O. Kaczmarek, F. Karsch, E. Laermann, C. Miao, S. Mukherjee, P. Petreczky, C. Schmidt, W. Soeldner, and W. Unger. Phase boundary for the chiral transition in (2+1) -flavor QCD at small values of the chemical potential. *Phys. Rev. D*, 83:014504, 2011.
- [4] J. Engels and F. Karsch. The scaling functions of the free energy density and its derivatives for the 3d O(4) model. *Phys. Rev. D*, 85:094506, 2012.
- [5] Florian Burger, Ernst-Michael Ilgenfritz, Malik Kirchner, Maria Paola Lombardo, Michael Müller-Preussker, Owe Philipsen, Carsten Urbach, and Lars Zeidlewicz. Thermal QCD transition with two flavors of twisted mass fermions. *Phys. Rev. D*, 87(7):074508, 2013.
- [6] A. Bazavov et al. Chiral crossover in QCD at zero and non-zero chemical potentials. *Phys. Lett. B*, 795:15–21, 2019.
- [7] H. T. Ding et al. Chiral Phase Transition Temperature in (2+1)-Flavor QCD. *Phys. Rev. Lett.*, 123(6):062002, 2019.
- [8] Frank R. Brown, Frank P. Butler, Hong Chen, Norman H. Christ, Zhi-hua Dong, Wendy Schaffer, Leo I. Unger, and Alessandro Vaccarino. On the existence of a phase transition for QCD with three light quarks. *Phys. Rev. Lett.*, 65:2491–2494, 1990.
- [9] Michael I. Buchoff et al. QCD chiral transition, U(1)A symmetry and the dirac spectrum using domain wall fermions. *Phys. Rev. D*, 89(5):054514, 2014.
- [10] Tanmoy Bhattacharya et al. QCD Phase Transition with Chiral Quarks and Physical Quark Masses. *Phys. Rev. Lett.*, 113(8):082001, 2014.
- [11] H. T. Ding, S. T. Li, Swagato Mukherjee, A. Tomiya, X. D. Wang, and Y. Zhang. Correlated Dirac Eigenvalues and Axial Anomaly in Chiral Symmetric QCD. *Phys. Rev. Lett.*, 126(8):082001, 2021.
- [12] Thomas D. Cohen. The High temperature phase of QCD and U(1)-A symmetry. *Phys. Rev. D*, 54:R1867–R1870, 1996.
- [13] Sinya Aoki, Hidenori Fukaya, and Yusuke Taniguchi. Chiral symmetry restoration, eigenvalue density of Dirac operator and axial U(1) anomaly at finite temperature. *Phys. Rev. D*, 86:114512, 2012.
- [14] Guido Cossu, Sinya Aoki, Hidenori Fukaya, Shoji Hashimoto, Takashi Kaneko, Hideo Matsufuru, and Jun-Ichi Noaki. Finite temperature study of the axial U(1) symmetry on the lattice with overlap fermion formulation. *Phys. Rev. D*, 87(11):114514, 2013. [Erratum: *Phys.Rev.D* 88, 019901 (2013)].
- [15] A. Tomiya, G. Cossu, S. Aoki, H. Fukaya, S. Hashimoto, T. Kaneko, and J. Noaki. Evidence of effective axial U(1) symmetry restoration at high temperature QCD. *Phys. Rev. D*, 96(3):034509, 2017. [Addendum: *Phys.Rev.D* 96, 079902 (2017)].
- [16] S. Aoki, Y. Aoki, G. Cossu, H. Fukaya, S. Hashimoto, T. Kaneko, C. Rohrhofer, and K. Suzuki. Study of the axial U(1) anomaly at high temperature with lattice chiral fermions. *Phys. Rev. D*, 103(7):074506, 2021.
- [17] Varouzhan Baluni. CP Violating Effects in QCD. *Phys. Rev. D*, 19:2227–2230, 1979.
- [18] Jihn E. Kim. Light Pseudoscalars, Particle Physics and Cosmology. *Phys. Rept.*, 150:1–177, 1987.
- [19] Mamiya Kawaguchi, Shinya Matsuzaki, and Akio Tomiya. Analysis of nonperturbative flavor violation at chiral crossover criticality in QCD. *Phys. Rev. D*, 103(5):054034, 2021.
- [20] A. Gómez Nicola and J. Ruiz de Elvira. Pseudoscalar susceptibilities and quark condensates: chiral restoration and lattice screening masses. *JHEP*, 03:186, 2016.

- [21] A. Gomez Nicola and J. Ruiz de Elvira. Patterns and partners for chiral symmetry restoration. Phys. Rev. D, 97(7):074016, 2018.
- [22] A. Gómez Nicola and J. Ruiz De Elvira. Chiral and $U(1)_A$ restoration for the scalar and pseudoscalar meson nonets. Phys. Rev. D, 98(1):014020, 2018.
- [23] Chuan-Xin Cui, Jin-Yang Li, Shinya Matsuzaki, Mamiya Kawaguchi, and Akio Tomiya. QCD trilemma. 6 2021.
- [24] Edward Witten. Current Algebra Theorems for the $U(1)$ Goldstone Boson. Nucl. Phys. B, 156:269–283, 1979.
- [25] G. Veneziano. $U(1)$ Without Instantons. Nucl. Phys. B, 159:213–224, 1979.
- [26] M. Kobayashi and T. Maskawa. Chiral symmetry and eta-x mixing. Prog. Theor. Phys., 44:1422–1424, 1970.
- [27] M. Kobayashi, H. Kondo, and T. Maskawa. Symmetry breaking of the chiral $u(3) \times u(3)$ and the quark model. Prog. Theor. Phys., 45:1955–1959, 1971.
- [28] Gerard 't Hooft. Symmetry Breaking Through Bell-Jackiw Anomalies. Phys. Rev. Lett., 37:8–11, 1976.
- [29] Gerard 't Hooft. Computation of the Quantum Effects Due to a Four-Dimensional Pseudoparticle. Phys. Rev. D, 14:3432–3450, 1976. [Erratum: Phys.Rev.D 18, 2199 (1978)].
- [30] S. P. Klevansky. The Nambu-Jona-Lasinio model of quantum chromodynamics. Rev. Mod. Phys., 64:649–708, 1992.
- [31] Tetsuo Hatsuda and Teiji Kunihiro. QCD phenomenology based on a chiral effective Lagrangian. Phys. Rept., 247:221–367, 1994.
- [32] T. Kunihiro. Chiral restoration, flavor symmetry and the axial anomaly at finite temperature in an effective theory. Nucl. Phys. B, 351:593–622, 1991.
- [33] K. Fukushima, K. Ohnishi, and K. Ohta. Topological susceptibility at zero and finite temperature in the Nambu-Jona-Lasinio model. Phys. Rev. C, 63:045203, 2001.
- [34] Yin Jiang and Pengfei Zhuang. Functional Renormalization for Chiral and $U_A(1)$ Symmetries at Finite Temperature. Phys. Rev. D, 86:105016, 2012.
- [35] Yin Jiang, Tao Xia, and Pengfei Zhuang. Topological Susceptibility in Three-Flavor Quark Meson Model at Finite Temperature. Phys. Rev. D, 93(7):074006, 2016.
- [36] Zhen-Yan Lu and Marco Ruggieri. Effect of the chiral phase transition on axion mass and self-coupling. Phys. Rev. D, 100(1):014013, 2019.
- [37] Angel Gómez Nicola, Jacobo Ruiz De Elvira, and Andrea Vioque-Rodríguez. The QCD topological charge and its thermal dependence: the role of the η' . JHEP, 11:086, 2019.
- [38] P. Di Vecchia and G. Veneziano. Chiral Dynamics in the Large n Limit. Nucl. Phys. B, 171:253–272, 1980.
- [39] F. C. Hansen and H. Leutwyler. Charge correlations and topological susceptibility in QCD. Nucl. Phys. B, 350:201–227, 1991.
- [40] H. Leutwyler and Andrei V. Smilga. Spectrum of Dirac operator and role of winding number in QCD. Phys. Rev. D, 46:5607–5632, 1992.
- [41] V. Bernard, S. Descotes-Genon, and G. Toucas. Determining the chiral condensate from the distribution of the winding number beyond topological susceptibility. JHEP, 12:080, 2012.
- [42] Feng-Kun Guo and Ulf-G. Meißner. Cumulants of the QCD topological charge distribution. Phys. Lett. B, 749:278–282, 2015.
- [43] Sz. Borsanyi et al. Calculation of the axion mass based on high-temperature lattice quantum chromodynamics. Nature, 539(7627):69–71, 2016.
- [44] Claudio Bonati, Massimo D’Elia, Guido Martinelli, Francesco Negro, Francesco Sanfilippo, and Antonino Todaro. Topology in full QCD at high temperature: a multicanonical approach. JHEP, 11:170, 2018.
- [45] Bastian B. Brandt, Anthony Francis, Harvey B. Meyer, Owe Philipsen, Daniel Robaina, and Hartmut Wittig. On the strength of the $U_A(1)$ anomaly at the chiral phase transition in $N_f = 2$ QCD. JHEP, 12:158, 2016.
- [46] Y. Aoki, Szabolcs Borsanyi, Stephan Durr, Zoltan Fodor, Sandor D. Katz, Stefan Krieg, and Kalman K. Szabo. The QCD transition temperature: results with physical masses in the continuum limit II. JHEP, 06:088, 2009.
- [47] Heng-Tong Ding, Frithjof Karsch, and Swagato Mukherjee. Thermodynamics of strong-interaction matter from Lattice QCD. Int. J. Mod. Phys. E, 24(10):1530007, 2015.
- [48] Peter Petreczky, Hans-Peter Schadler, and Sayantan Sharma. The topological susceptibility in finite temperature QCD and axion cosmology. Phys. Lett. B, 762:498–505, 2016.